Article

A two-way molecular dialogue between embryo and endosperm is required for seed development

DOLL, N M, *et al*.

Abstract

The plant embryonic cuticle is a hydrophobic barrier deposited de novo by the embryo during seed development. At germination, it protects the seedling from water loss and is, thus, critical for survival. Embryonic cuticle formation is controlled by a signaling pathway involving the ABNORMAL LEAF SHAPE1 subtilase and the two GASSHO receptor-like kinases. We show that a sulfated peptide, TWISTED SEED1 (TWS1), acts as a GASSHO ligand. Cuticle surveillance depends on the action of the subtilase, which, unlike the TWS1 precursor and the GASSHO receptors, is not produced in the embryo but in the neighboring endosperm. Subtilase-mediated processing of the embryo-derived TWS1 precursor releases the active peptide, triggering GASSHO-dependent cuticle reinforcement in the embryo. Thus, a bidirectional molecular dialogue between embryo and endosperm safeguards cuticle integrity before germination.

Reference

DOLL, N M, *et al*. A two-way molecular dialogue between embryo and endosperm is required for seed development. *Science*, 2020, vol. 367, no. 6476, p. 431-435

DOI : 10.1126/science.aaz4131
PMID : 31974252

Title: A two-way molecular dialogue between embryo and endosperm required for seed development

Authors: N. M. Doll[1], S. Royek[2,†], S. Fujita[3,†,‡], S. Okuda[4,†], S. Chamot[1], A. Stintzi[2], T. Widiez[1], M. Hothorn[4], A. Schaller[2], N. Geldner[3], G. Ingram[1,*]

Affiliations:

[1]Laboratoire Reproduction et Développement des Plantes, University of Lyon, ENS de Lyon, UCB Lyon 1, CNRS, INRA, F-69342, Lyon, France.

[2]Department of Plant Physiology and Biochemistry, University of Hohenheim, Stuttgart, Germany.

[3]Department of Plant Molecular Biology, University of Lausanne, 1015 Lausanne, Switzerland.

[4]Structural Plant Biology Laboratory, Department of Botany and Plant Biology, University of Geneva, 1211 Geneva, Switzerland.

*Correspondence to: gwyneth.ingram@ens-lyon.fr.

†equal contribution

‡current address: National Institute of Genetics, 1111 Yata, Mishima, Shizuoka 411-8540, Japan.

Abstract (129 words)**:** The plant embryonic cuticle is a hydrophobic barrier deposited *de novo* by the embryo during seed development. At germination it protects the seedling from water loss and is thus critical for survival. Embryonic cuticle formation is controlled by a signaling pathway involving the ABNORMAL LEAF SHAPE1 subtilase, and the two GASSHO receptor-like kinases. We show that a sulfated peptide, TWISTED SEED1 (TWS1), acts as a GASSHO ligand. Cuticle surveillance depends on the action of the subtilase which, unlike the TWS1 precursor and the GASSHO receptors, is not produced in the embryo but in the neighboring endosperm. Subtilase-mediated processing of the embryo-derived TWS1 precursor releases the active peptide, triggering GASSHO-dependent cuticle reinforcement in the embryo. A bidirectional molecular dialogue between embryo and endosperm thus safeguards cuticle integrity prior to germination.

One Sentence Summary: Compartmentalized proteolytic activation of a signal peptide provides spatial cues to ensure an intact embryo cuticle.

Main Text (2047 words): In Angiosperms, seeds comprise three genetically distinct compartments, the zygotic embryo and the endosperm, and the maternal seed coat. Their development must be tightly coordinated for seed viability. Here we have elucidated a bidirectional peptide-mediated signaling pathway between the embryo and the endosperm. This pathway regulates the deposition of the embryonic cuticle which forms an essential hydrophobic barrier separating the apoplasts of the embryo and endosperm. After germination, the cuticle - one of the critical innovations underlying the transition of plants from their original, aqueous environment to dry land - protects the seedling from catastrophic water loss (*1*, *2*).

Formation of the embryonic cuticle was previously shown to depend on two Receptor-Like Kinases (RLKs) GASSHO1/SCHENGEN3 (from here-on named GSO1) and GSO2, and on ALE1, a protease of the subtilase family (SBTs) (*2–5*). *gso1 gso2* and (to a lesser extent) *ale1* mutants produce a patchy, and highly permeable cuticle (*2*). Mutant embryos also adhere to surrounding tissues causing a seed-twisting phenotype (*6*). Since SBTs have been implicated in the processing of peptide hormone precursors (*7*, *8, 9*), we hypothesized that ALE1 may be required for the biogenesis of the elusive inter-compartmental peptide signal required for GSO1/2-dependent cuticle deposition.

CASPARIAN STRIP INTEGRITY FACTORs (CIFs), a family of small sulfated signaling peptides, are ligands for GSO1 and GSO2 (*10–12*). CIF1 and CIF2 are involved in Casparian strip formation in the root endodermis (*10*, *11*). The function of CIF3 and CIF4 is still unknown. To assess the role of CIF peptides in cuticle development, the quadruple mutant (*cif1 cif2 cif3 cif4)* was generated (Fig. S1A). Neither cuticle permeability nor seed twisting phenotypes were

observed in this quadruple mutant (Fig. S1B-E). However, reduction (in the leaky *sgn2-1* allele (*10*)) or loss (in the *tpst-1* mutant (*13*)) of Tyrosyl-Protein Sulfotransferase (TPST) activity, results in seed-twisting and cuticle-permeability phenotypes resembling those observed in *ale1* mutants (Fig. 1A-D, Fig. S2 A-D). These data suggest that a sulfated peptide may act as the ligand of GSO1/2 during seed development.

Consistent with the hypothesis that TPST acts in the same pathway as GSO1 and GSO2, no difference was observed between the phenotype of *tpst-1 gso1-1 gso2-1* triple and *gso1-1 gso2-1* double mutants (Fig. S2E). In contrast, TPST and ALE1 appear to act synergistically, as a phenotype resembling that of *gso1 gso2* double mutants was observed in *tpst-1 ale1-4* double mutants (Fig. 1E-I) (Fig. S2F-J). This result supports the hypothesis that TPST and ALE1 act in parallel regarding their roles in embryonic cuticle formation, possibly through independent post-translational modifications contributing to the maturation of the hypothetical peptide signal.

Identification of the peptide signal was facilitated by a study of TWISTED SEED1 (TWS1) (*14*), that reported a loss-of-function phenotype strikingly similar to that of *gso1 gso2* double mutants. Because existing alleles of *TWS1* are in the WS background, we generated new CRISPR alleles (*tws1-3* to *tws1-10)* in the Col-0 background, and confirmed the phenotype of resulting mutants (Fig. 1, Fig. S3). No additivity was observed when loss-of-function alleles of *TWS1* and of other pathway components (*GSO1, GSO2, TPST* and *ALE1*) were combined, providing genetic evidence for *TWS1* acting in the GSO signaling pathway (Fig. S4). Furthermore, gaps in the cuticle of embryos and cotyledons similar to those observed in *ale1* and *gso1 gso2* mutants *(2),* were detected in both the *tws1* mutants and *tpst* mutants (Fig. 1 J-N, Fig. S5). Inspection of the TWS1 protein sequence revealed a region with limited similarity to CIF peptides including a DY motif which marks the N-terminus of the CIFs (Fig. 1O), and is the minimal motif required for tyrosine sulfation

by TPST (*15*). Corroborating the functional importance of the putative peptide domain, the *tws1-6* allele (deletion of six codons in the putative peptide-encoding region) and the *tws1-5* allele (substitution of eight amino acids including the DY motif) both showed total loss of function of the TWS1 protein (Fig. S3).

We tested whether TWS1 is a substrate of ALE1 by co-expression of ALE1:(His)6 and TWS1:GFP-(His)6 fusion proteins in tobacco (*N. benthamiana*) leaves. A specific TWS1 cleavage product was observed upon co-expression of ALE1 but not in the empty-vector control suggesting that TWS1 is processed by ALE1 *in planta* (Fig. 1P). Likewise, recombinant TWS1 expressed as GST-fusion in *E. coli* was cleaved by purified ALE1 *in vitro*. (Fig. 1Q). Mass spectroscopy analysis of the TWS1 cleavage product purified from tobacco leaves showed that ALE1 cleaves TWS1 between His_{54} and Gly_{55} (Fig. S6). These residues are important for cleavage site selection, as ALE1-dependent processing was not observed when either His_{54} or Gly_{55} was substituted by site-directed mutagenesis (Fig. 1Q). His_{54} corresponds to the C-terminal His or Asn of CIF peptides (Fig. 1O). The data thus suggest that ALE1-mediated processing of the TWS1 precursor marks the C-terminus of the TWS1 peptide. Because the CIF1 and CIF2 peptides are located at the very end of their respective precursors, C-terminal processing could represent a mechanism of peptide activation operating in the developing seed but not in the root. A summary of TWS1 modifications is provided in Fig. 1R.

To test the biological activity of TWS1, the predicted peptide encompassing the conserved N-terminal DY-motif and the C-terminus defined by the ALE1 cleavage site was custom-synthesized in tyrosine-sulfated form. As synthetic TWS1 cannot easily be applied to developing embryos, a root bioassay for CIF activity was used. In wild-type roots TWS1 induced ectopic endodermal lignification as previously observed for the CIF1 and CIF2 peptides (*12*). TWS1 activity was

GSO1-dependent, suggesting that processed TWS1 peptide can replace CIF1 and CIF2 as a ligand for GSO1 during Casparian strip formation (Fig. 2A) (Fig. S7). Supporting this, TWS1 application complemented the *cif1 cif2* mutant, albeit with reduced activity compared to CIF2 (Fig. 2B, Fig. S8). TWS1 activity in this assay was reduced when sulfation on the DY motif was missing (Fig. 2B). Versions of TWS1 in which Y_{33} was mutated to either F or T only partially complemented the mutant phenotype of *tws1-4* (Fig S9), consistent with a residual but weak activity for non-sulfated TWS1 *in vivo*, and with the weak loss-of-function phenotype of the *tpst-1* mutant.

To confirm TWS1 as a ligand of GSO1 and GSO2, the interaction of the synthetic peptide with the leucine-rich repeat (LRR) ectodomains of the receptors was analyzed in grating – coupled interferometry binding assays. GSO1 bound sulfated TWS1 with a K_D of ~ 30 nM (Fig. 2C). The observed binding affinity is ~10 fold lower compared to the CIF2 peptide (K_D = 2.5 nM) (Fig. S10), which is consistent with the reduced ability of TWS1 to complement the root phenotype of the *cif1 cif2* double mutant (Fig. 2B). Sulfated TWS1 also bound to the LRR domain of GSO2, albeit with slightly reduced affinity (K_D ~ 100 nM) (Fig.2D). As previously shown for other CIF peptides (*11*), tyrosine sulfation was critical for the interaction of TWS1 with GSO1 and GSO2 *in vitro* (Fig. 2E,F). Technical issues at high peptide concentrations may explain discrepancies between *in vitro* binding assays and the *in vivo* activity of non-sulfated TWS1. *In vivo* activities for non-sulfated versions of other normally-sulfated peptides, including CIF2, have been reported *(11,16-18)*. Adding a 3AA C-terminal extension to the sulfated TWS1 peptide reduced binding affinity to both GSO1 and GSO2 (Fig. S10), consistent with the need for ALE1-mediated C-terminal processing for efficient signaling.

Taken together, our results suggest the sulfated TWS peptide as the missing link in the inter-compartmental signaling pathway for embryonic cuticle formation. The activities of ALE1 and

TPST both contribute to the formation of the bioactive peptide (Fig. 1R) which is perceived by GSO1 and GSO2 to ensure appropriate cuticle deposition.

To understand how the elements of the signaling pathway cooperate to ensure the formation of a functional cuticle, we analyzed their spatial organization. *In silico* data indicate that the *TPST* gene is expressed in all seed tissues (Fig. S11) (*19*, *20*). To investigate in which compartment TPST (which acts cell autonomously (*13*)) is required for TWS1 maturation, reciprocal crosses and complementation assays using tissue specific promoters were performed. No cuticle permeability defects were observed when homozygous mutants were pollinated with wild-type pollen, confirming their zygotic origin. (Fig. 3A-C). Expressing TPST under the ubiquitously active *RPS5A* promoter (*21*), or the *PIN1* promoter (which is embryo-specific in seed (Fig. S12)) complements *tpst-1* cuticle defects. In contrast no complementation was observed using the endosperm-specific *RGP3* promoter (*22*), indicating that TPST activity is required for TWS1 sulfation specifically in the embryo to ensure cuticle integrity (Fig. 3D) (Fig. S13). Consistent with this observation, and with a previous report (*14*), the *TWS1* promoter was found to drive expression specifically in the developing embryo from the early globular stage onwards (Fig. 3E) (Fig S14). The *TPST* promoter (*10*) drove expression throughout the embryo proper at the onset of embryo cuticle establishment (globular stage) before becoming restricted to the root tip (Fig. S11). We conclude that the TWS1 peptide is both sulfated and secreted specifically in the embryo.

However, production of mature TWS1 requires a C-terminal cleavage event that we have shown to be mediated by ALE1. *ALE1* is expressed only in the endosperm (*4*, *23*), on the opposite side of the nascent cuticle to the GSO1 and GSO2 receptors, which are localized on the membranes of the epidermal cells that produce the cuticle (Fig. S15-17) *(2)*. Our data thus support a model in which activation of the GSO signaling pathway depends on the diffusion of the TWS1 peptide precursor

to the endosperm, where it is cleaved and activated by ALE1 before diffusing back to the embryo to trigger GSO1/2-dependent cuticle deposition. An intact cuticle would separate the subtilase from its substrate, terminating signaling.

Expressing *ALE1* in the embryo, under the control of the *TWS1* promoter, provided support for this model. Multiple transformants were obtained in *tws1* mutants, but not in the wild-type background. When *tws1* plants carrying the *pTWS1:ALE1* transgene were pollinated with wild-type pollen, introducing a functional *TWS1* allele into the zygotic compartments, and thus inducing colocalization of TWS1 precursors, ALE1, GSO1 and GSO2 in the embryo, premature embryo growth arrest was observed (Fig. 3F-M) (Fig. S18, S19). A proportion of seeds could nonetheless germinate to give developmentally normal plants (Fig. S20) indicating that co-expression of all signaling components in the embryo is detrimental to embryo development. This may be due to constitutive embryonic activation of the *GSO1/GSO2* signaling pathway, and indeed stress-responsive genes shown to require GSO1/GSO2 signaling for expression in the seed (*2*) were upregulated in seeds co-expressing GSO1, GSO2, TWS1 and ALE1 in the embryo (Fig. S21). We thus postulate that the spatial separation of the TWS1 precursor and the GSO receptors from the activating protease by cuticle is required for signaling attenuation.

We next tested if CIF1, CIF2 and TWS1 could complement *tws1* and *ale1* mutants when expressed in the endosperm (under the *RGP3* promoter). All three peptides complemented *tws1* mutants, confirming that retrograde peptide movement from endosperm to embryo is sufficient to allow integrity monitoring (Fig. 3N and Fig. S22). Lack of full complementation could reflect suboptimal N-terminal processing or sulfation in the endosperm. CIF1 and CIF2 (lacking C-terminal extensions) complemented *ale1* mutants much more efficiently than TWS1 (Fig. S23). Weak

complementation of *ale1* by TWS1 may reflect the presence of redundantly-acting subtilases in the endosperm, as suggested by the weak phenotype of *ale1* mutants.

The proposed bidirectional signaling model allows efficient embryo cuticle integrity monitoring. The sulfated TWS1 precursor is produced by the embryo and secreted (probably after N-terminal cleavage of the pro-peptide) to the embryo apoplast. In the absence of an intact cuticular barrier, it can diffuse to the endosperm and undergo activation by ALE1 (and potentially other subtilases). Activated TWS1 peptide then leaks back through cuticle gaps to bind the GSO1 and GSO2 receptors and activate local gap repair (Fig. 3O). When the cuticle is intact, proTWS1 peptides are confined to the embryo where they remain inactive.

Our results demonstrate a role for a subtilase in providing spatial specificity to a bidirectional peptide signaling pathway. In contrast, the related CIF1, CIF2 and GSO1-dependent signaling pathway controlling Casparian strip integrity is uni-directional, negating the need for C-terminal cleavage-mediated peptide activation (*10*, *12*). Both pathway components and their spatial organization differ between the two systems, suggesting an independent recruitment of the GSO receptors to different integrity monitoring functions within the plant.

References and Notes:

1. C. Delude, S. Moussu, J. Joubès, G. Ingram, F. Domergue, Plant Surface Lipids and Epidermis Development. Subcell. Biochem. 86, 287–313 (2016).

2. A. Creff, L. Brocard, J. Joubès, L. Taconnat, N. M. Doll, A.-C. Marsollier, S. Pascal, R. Galletti, S. Boeuf, S. Moussu, T. Widiez, F. Domergue, G. Ingram, A stress-response-related inter-compartmental signalling pathway regulates embryonic cuticle integrity in Arabidopsis. PLoS Genet. 15, e1007847 (2019).

3. R. Tsuwamoto, H. Fukuoka, Y. Takahata, GASSHO1 and GASSHO2 encoding a putative leucine-rich repeat transmembrane-type receptor kinase are essential for the normal development of the epidermal surface in Arabidopsis embryos. Plant J. Cell Mol. Biol. 54, 30–42 (2008).

4. H. Tanaka, H. Onouchi, M. Kondo, I. Hara-Nishimura, M. Nishimura, C. Machida, Y. Machida, A subtilisin-like serine protease is required for epidermal surface formation in Arabidopsis embryos and juvenile plants. Dev. Camb. Engl. 128, 4681–4689 (2001).

5. Q. Xing, A. Creff, A. Waters, H. Tanaka, J. Goodrich, G. C. Ingram, ZHOUPI controls embryonic cuticle formation via a signalling pathway involving the subtilisin protease ABNORMAL LEAF-SHAPE1 and the receptor kinases GASSHO1 and GASSHO2. Dev. Camb. Engl. 140, 770–779 (2013).

6. S. Moussu, N. M. Doll, S. Chamot, L. Brocard, A. Creff, C. Fourquin, T. Widiez, Z. L. Nimchuk, G. Ingram, ZHOUPI and KERBEROS Mediate Embryo/Endosperm Separation by Promoting the Formation of an Extracuticular Sheath at the Embryo Surface. Plant Cell. 29, 1642–1656 (2017).

7. A. Schaller, A. Stintzi, S. Rivas, I. Serrano, N. V. Chichkova, A. B. Vartapetian, D. Martínez, J. J. Guiamét, D. J. Sueldo, R. A. L. van der Hoorn, V. Ramírez, P. Vera, From structure to function - a family portrait of plant subtilases. New Phytol. 218, 901–915 (2018).

8. N. Stührwohldt, A. Schaller, Regulation of plant peptide hormones and growth factors by post-translational modification. Plant Biol. (Suppl 1), 49–63 (2019).

9. K. Schardon, M. Hohl, L. Graff, J. Pfannstiel, W. Schulze, A. Stintzi, A. Schaller, Precursor processing for plant peptide hormone maturation by subtilisin-like serine proteinases. Science. 354, 1594–1597 (2016).

10. V. G. Doblas, E. Smakowska-Luzan, S. Fujita, J. Alassimone, M. Barberon, M. Madalinski, Y. Belkhadir, N. Geldner, Root diffusion barrier control by a vasculature-derived peptide binding to the SGN3 receptor. Science. 355, 280–284 (2017).

11. S. Okuda, S. Fujita, A. Moretti, U. Hohmann, V. Gonzalez Doblas, Y. Ma, A. Pfister, B. Brandt, N. Geldner, M. Hothorn, Molecular mechanism for the recognition of sequence-divergent CIF peptides by the plant receptor kinases GSO1/SGN3 and GSO2. bioRxiv, 692228.

12. T. Nakayama, H. Shinohara, M. Tanaka, K. Baba, M. Ogawa-Ohnishi, Y. Matsubayashi, A peptide hormone required for Casparian strip diffusion barrier formation in Arabidopsis roots. Science. 355, 284–286 (2017).

13. R. Komori, Y. Amano, M. Ogawa-Ohnishi, Y. Matsubayashi, Identification of tyrosylprotein sulfotransferase in Arabidopsis. Proc. Natl. Acad. Sci. U. S. A. 106, 15067–15072 (2009).

14. E. Fiume, V. Guyon, C. Remoué, E. Magnani, M. Miquel, D. Grain, L. Lepiniec, TWS1, a Novel Small Protein, Regulates Various Aspects of Seed and Plant Development. Plant Physiol. 172, 1732–1745 (2016).

15. H. Hanai, D. Nakayama, H. Yang, Y. Matsubayashi, Y. Hirota, Y. Sakagami, Existence of a plant tyrosylprotein sulfotransferase: novel plant enzyme catalyzing tyrosine O-sulfation of preprophytosulfokine variants in vitro. FEBS Lett. 470, 97–101 (2000).

16. Y. Matsubayashi, Y. Sakagami, Characterization of specific binding sites for a mitogenic sulfated peptide, phytosulfokine-alpha, in the plasma-membrane fraction derived from Oryza sativa L. Eur. J. Biochem. 262, 666–671 (1999).

17. A. Kutschmar, G. Rzewuski, N. Stührwohldt, G. T. S. Beemster, D. Inzé, M. Sauter, PSK-α promotes root growth in Arabidopsis. New Phytol. 181, 820–831 (2009).

18. Y. Matsuzaki, M. Ogawa-Ohnishi, A. Mori, Y. Matsubayashi, Secreted peptide signals required for maintenance of root stem cell niche in Arabidopsis. Science. 329, 1065–1067 (2010).

19. B. H. Le, C. Cheng, A. Q. Bui, J. A. Wagmaister, K. F. Henry, J. Pelletier, L. Kwong, M. Belmonte, R. Kirkbride, S. Horvath, G. N. Drews, R. L. Fischer, J. K. Okamuro, J. J. Harada, R. B. Goldberg, Global analysis of gene activity during Arabidopsis seed development and identification of seed-specific transcription factors. Proc. Natl. Acad. Sci. U. S. A. 107, 8063–8070 (2010).

20. A. V. Klepikova, A. S. Kasianov, E. S. Gerasimov, M. D. Logacheva, A. A. Penin, A high resolution map of the Arabidopsis thaliana developmental transcriptome based on RNA-seq profiling. Plant J. Cell Mol. Biol. 88, 1058–1070 (2016).

21. D. Weijers, Franke-van Dijk, M., R. J. Vencken, Quint, A., Hooykaas, P., Offringa, R., An Arabidopsis Minute-like phenotype caused by a semi-dominant mutation in a RIBOSOMAL PROTEIN S5 gene. Dev. Camb. Engl. 128, 4289–4299 (2001).

22. G. Denay, A. Creff, S. Moussu, P. Wagnon, J. Thévenin, M.-F. Gérentes, P. Chambrier, B. Dubreucq, G. Ingram, Endosperm breakdown in Arabidopsis requires heterodimers of the basic helix-loop-helix proteins ZHOUPI and INDUCER OF CBP EXPRESSION 1. Dev. Camb. Engl. 141, 1222–1227 (2014).

23. S. Yang, N. Johnston, E. Talideh, S. Mitchell, C. Jeffree, J. Goodrich, G. Ingram, The endosperm-specific ZHOUPI gene of Arabidopsis thaliana regulates endosperm breakdown and embryonic epidermal development. Dev. Camb. Engl. 135, 3501–3509 (2008).

24. A. Pfister, M. Barberon, J. Alassimone, L. Kalmbach, Y. Lee, J. E. M. Vermeer, M. Yamazaki, G. Li, C. Maurel, J. Takano, T. Kamiya, D. E. Salt, D. Roppolo, N. Geldner, A receptor-like kinase mutant with absent endodermal diffusion barrier displays selective nutrient homeostasis defects. eLife. 3, e03115 (2014).

25. D. Roppolo, B. De Rybel, V. D. Tendon, A. Pfister, J. Alassimone, J. E. M. Vermeer, M. Yamazaki, Y.-D. Stierhof, T. Beeckman, N. Geldner, A novel protein family mediates Casparian strip formation in the endodermis. Nature. 473, 380–383 (2011).

26. J. Friml, A. Vieten, M. Sauer, D. Weijers, H. Schwarz, T. Hamann, R. Offringa, G. Jürgens, Efflux-dependent auxin gradients establish the apical–basal axis of Arabidopsis. Nature. 426, 147 (2003).

27. Z.-P. Wang, H.-L. Xing, L. Dong, H.-Y. Zhang, C.-Y. Han, X.-C. Wang, Q.-J. Chen, Egg cell-specific promoter-controlled CRISPR/Cas9 efficiently generates homozygous mutants for multiple target genes in Arabidopsis in a single generation. Genome Biol. 16, 144 (2015).

28. F. Fauser, S. Schiml, H. Puchta, Both CRISPR/Cas-based nucleases and nickases can be used efficiently for genome engineering in Arabidopsis thaliana. Plant J. 79, 348–359 (2014).

29. E. Logemann, R. P. Birkenbihl, B. Ülker, I. E. Somssich, An improved method for preparing Agrobacterium cells that simplifies the Arabidopsis transformation protocol. Plant Methods. 2, 16 (2006).

30. T. Tanaka, H. Tanaka, C. Machida, M. Watanabe, Y. Machida, A new method for rapid visualization of defects in leaf cuticle reveals five intrinsic patterns of surface defects in Arabidopsis. Plant J. 37, 139–146 (2004).

31. U. Roshan, D. R. Livesay, Probalign: multiple sequence alignment using partition function posterior probabilities. Bioinforma. Oxf. Engl. 22, 2715–2721 (2006).

32. D. Kurihara, Y. Mizuta, Y. Sato, T. Higashiyama, ClearSee: a rapid optical clearing reagent for whole-plant fluorescence imaging. Development. 142, 4168–4179 (2015).

33. R. Ursache, T. G. Andersen, P. Marhavý, N. Geldner, A protocol for combining fluorescent proteins with histological stains for diverse cell wall components. Plant J. 93, 399–412 (2018).

34. R Core Team, R: A language and environment for statistical computing. R Foundation for Statistical Computing, Vienna, Austria. (2013).

35. Y. Hashimoto, S. Zhang, G. W. Blissard, Ao38, a new cell line from eggs of the black witch moth, Ascalapha odorata (Lepidoptera: Noctuidae), is permissive for AcMNPV infection and produces high levels of recombinant proteins. BMC Biotechnol. 10, 50 (2010).

36. M. Fairhead, M. Howarth, Site-specific biotinylation of purified proteins using BirA. Methods Mol. Biol. Clifton NJ. 1266, 171–184 (2015).

37. A. P. Gleave, A versatile binary vector system with a T-DNA organisational structure conducive to efficient integration of cloned DNA into the plant genome. Plant Mol. Biol. 20, 1203–1207 (1992).

38. A. Shevchenko, M. Wilm, O. Vorm, M. Mann, Mass spectrometric sequencing of proteins silver-stained polyacrylamide gels. Anal. Chem. 68, 850–858 (1996).

39. J. V. Olsen, L. M. F. de Godoy, G. Li, B. Macek, P. Mortensen, R. Pesch, A. Makarov, O. Lange, S. Horning, M. Mann, Parts per million mass accuracy on an Orbitrap mass spectrometer via lock mass injection into a C-trap. Mol. Cell. Proteomics MCP. 4, 2010–2021 (2005).

Acknowledgments: We thank Loïc Lepiniec for providing the *tws1-1* and *tws1-2* seeds, Carlos Galvan Ampudia, Yvon Jaillais and Laia Armengot for materials and helpful discussions, Audrey Creff, Ursula Glück-Behrens, Alexis Lacroix, Patrice Bolland, Justin Berger, Isabelle Desbouchages and Hervé Leyral for technical assistance, Angélique Patole, Brigitte Martin Sempore, Cindy Vial and Stéphanie Maurin for administrative assistance and Berit Würtz and Jens Pfannstiel (Core Facility Hohenheim) for mass spectrometric analyses. TEM images were acquired at the Centre Technologique des Microstructures, Université Lyon1.

Funding: The study was financed by joint funding (project Mind the Gap) from the French Agence National de Recherche (ANR- 17-CE20-0027) (G.I.) and the Swiss National Science Foundation (NSF) (N.G., supporting S.F.). N.M.D. was funded by a PhD fellowship from the Ministère de l'Enseignement Supérieur et de la Recherche. Funding was also provided by NSR grant no 31003A_176237 (M.H.) and an International Research Scholar grant from the Howard Hughes Medical Institute (to M.H). S.O. was supported by a long-term postdoctoral fellowship by the Human Frontier Science Program (HFSP). S.R. was supported by a PhD fellowship from the Carl-Zeiss Foundation.

Author contributions: G.I. led the study. G.I. and N.G. obtained funding for the study. G.I., N.G., A.Sc., M.H. T.W and A.St. supervised the work. N.M.D., S.R., S.F., S.O. and S.C. carried out the experiments. All authors were involved in the analysis of the results. G.I., A.Sc. and N.M.D. wrote the paper with input from all authors.

Competing interests: The authors declare no competing interests.

Data and materials availability: All lines used in the study will be provided upon signature of an appropriate Material Transfer Agreement. All data is available in the main text or the supplementary materials.

Supplementary Materials:

Materials and Methods

Figures S1-S23

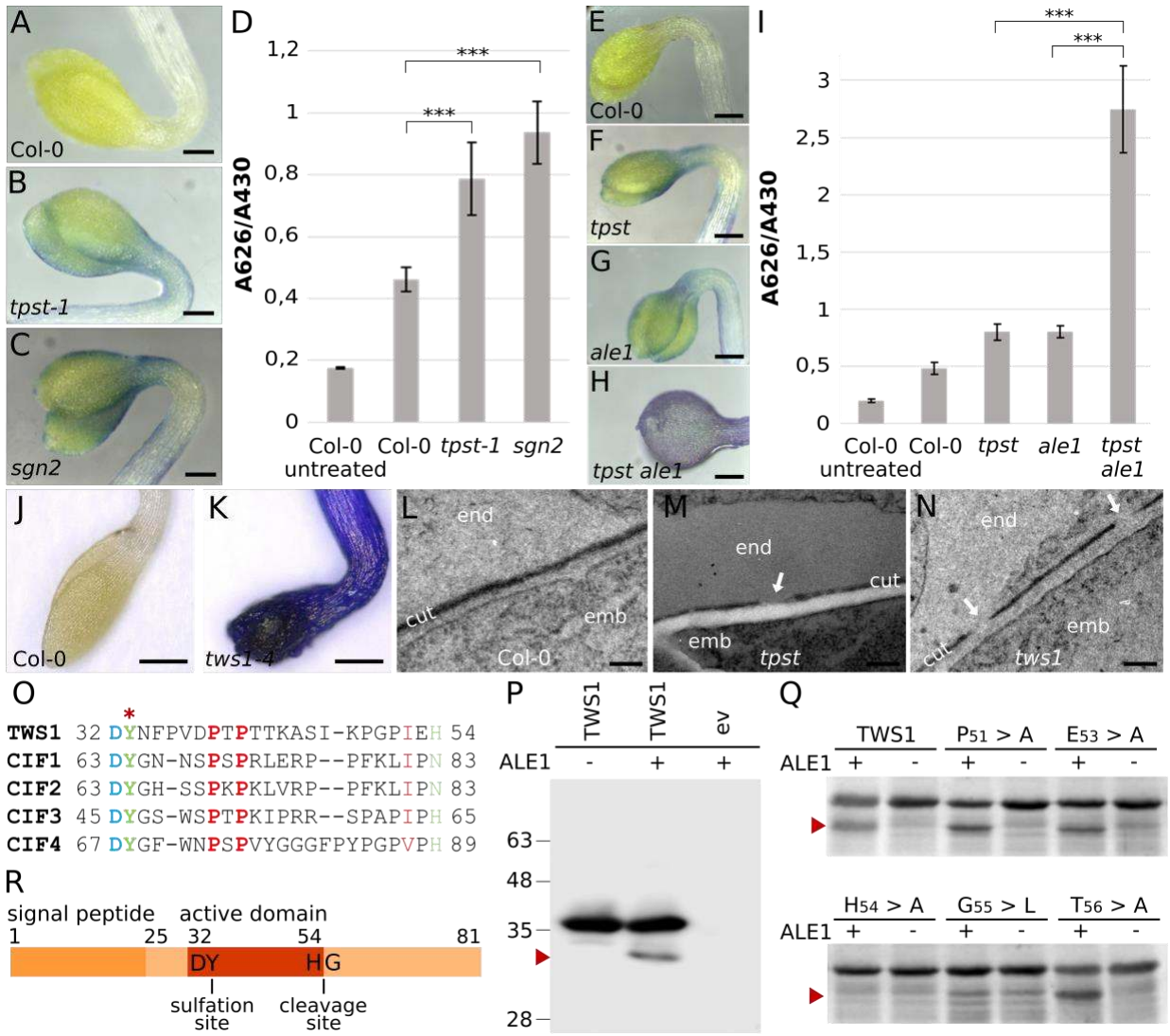

Fig. 1. TPST and ALE1 are required for maturation of the TWS1 peptide. A-C, E-H and J-K) Toluidine blue tests on etiolated cotyledons. Scale bars = 200µm. D and I) Quantification of toluidine blue uptake by the aerial parts of young seedlings, normalized to chlorophyll content. N=6, ten seedlings per repetition. *** = statistical differences with one-way ANOVA followed by a *post-hoc* Scheffé multiple comparison test (P < 0,01) in D and I. J and K) Toluidine blue permeability of *tws1-4* compared to Col-0. Scale bars = 400µm L-M) Transmission electron micrographs of the embryo/endosperm interface at the heart stage. Scale bars = 200nm. Genotypes are indicated, and gaps in the cuticle are shown by white arrows. O) The predicted TWS1 active peptide sequence and alignment with four other known GSO ligands (CIF1,CIF2, CIF3 and CIF4). The site of predicted sulfation is indicated with a red asterisk. P) Anti-His western blot of protein extracts from *N. benthamiana* leaves agro-infiltrated to express TWS1::GFP(His)6 (TWS1) or the

empty vector (-). Co-expression of ALE1::(His)6 or the empty-vector control are indicated by + and -, respectively. Q) Coomassie-stained SDS-PAGE showing recombinant GST-TWS1 and the indicated site-directed mutants digested *in vitro* with (+) or without (-) ALE1-(His)6 purified from tobacco leaves. Arrows indicate specific cleavage products. R) The full length TWS1 precursor. Sulfation and ALE1 cleavage sites are indicated.

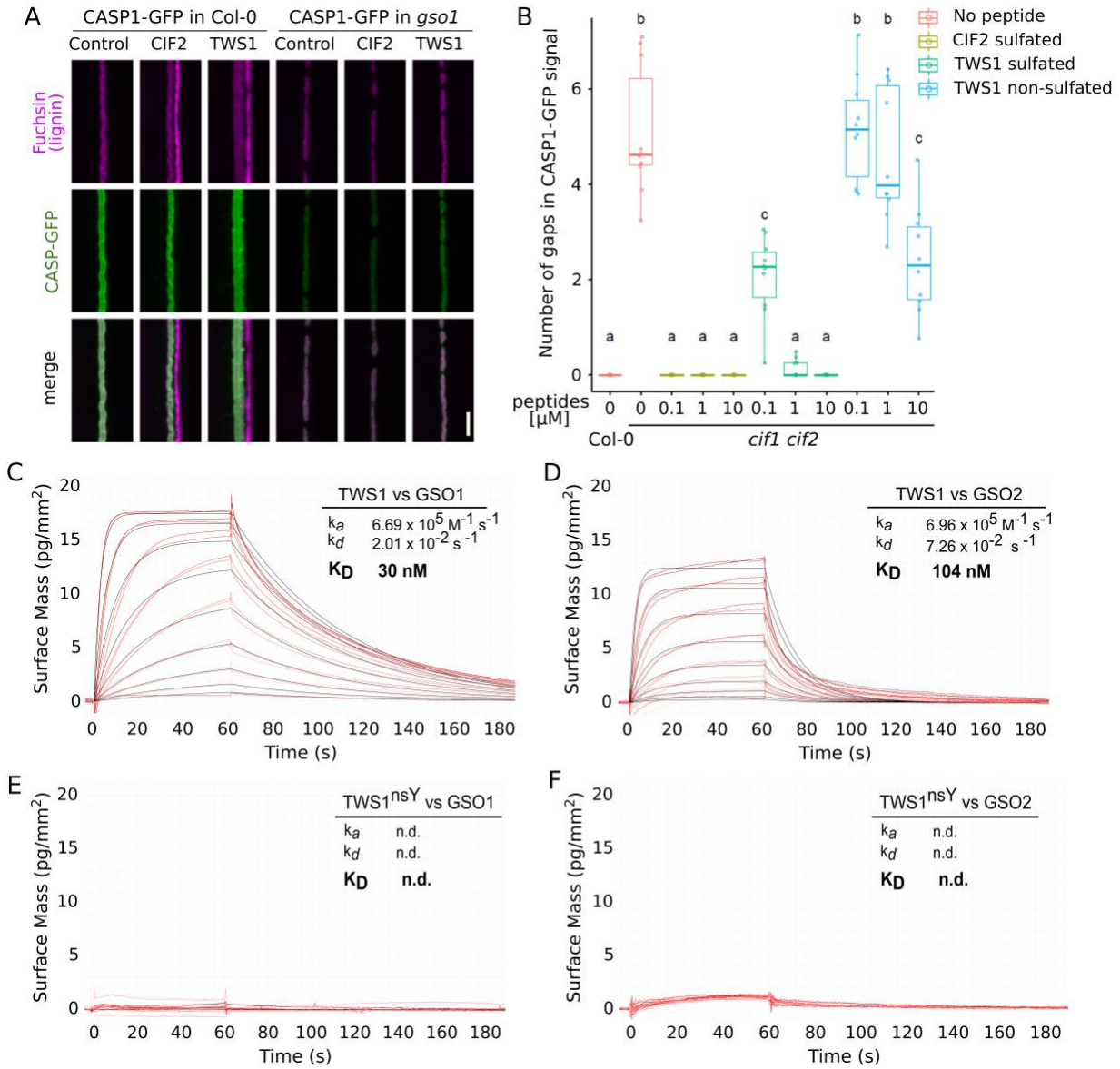

Fig. 2. The TWS1 peptide is a functional GSO1/GSO2 ligand. A) Root over-lignification following treatment with the active CIF2 or TWS peptide in Col-0 and in the *gso1 (sgn3-3)* background. Lignin is stained in purple and CASP-GFP fusion protein, marking the Casparian strip domain, in green. Scale bar = 5µm B) Complementation of *cif1-2 cif2-2* Casparian strip integrity phenotype by peptide treatments. Number of gaps in CASP1-GFP signal counted after treatment with CIF2 sulfated peptide, TWS1 sulfated peptide, TWS1 non-sulfated peptide. N=10. a, b, and c correspond to a classes statistically supported by one-way ANOVA analysis followed by Tukey tests (P < 0,05). C-F) Grating-coupled interferometry (GCI)-derived binding kinetics. Shown are sensorgrams with raw data in red and their respective fits in black. k_a, association rate

constant; k_d, dissociation rate constant; K_D, dissociation constant. C) on the GSO1 extra-cellular domain in the presence of the sulfated TWS1 peptide. D) on the GSO2 extra-cellular domain in the presence of the sulfated TWS1 peptide. E) on the GSO1 extra-cellular domain in the presence of the non-sulfated TWS1 peptide. F) on the GSO2 extra-cellular domain in the presence of the non-sulfated TWS1 peptide.

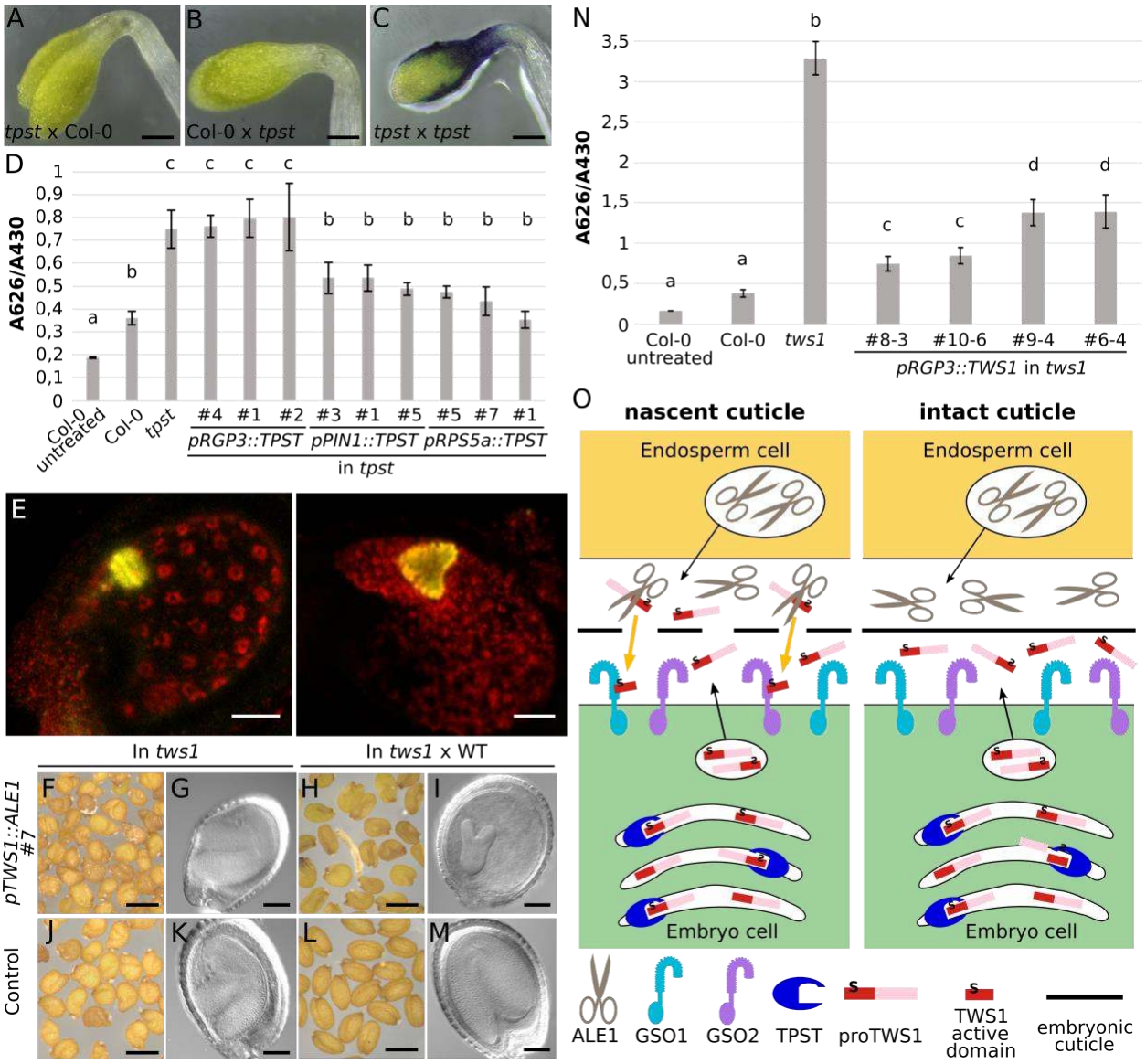

Fig. 3. Spatial separation of *ALE1* and *TWS1* expression is critical for pathway function. A-C) F1 seedlings from reciprocal crosses stained with Toluidine blue. D,N) Toluidine blue quantification as in Fig. 1. a-d = statistical differences with one-way ANOVA followed by a *post-hoc* Scheffé multiple comparison test (P < 0,01). D) Complementation of *tpst-1* mutant with endosperm-specific expression of *TPST* (*pRGP3::TPST*), embryo-specific expression of *TPST (pPIN1:TPST)* and ubiquitous expression of *TPST (pRPS5a::TPST)* compared to *tpst-1* and Col-0. 3 independent lines were analysed. E) Confocal images of *pTWS1::mCitrine::NLS-mCitrine* reporter lines, signal in yellow, autofluorescence in red. Scale bars = 50µm. F,G) Dry seeds (scale

bars = 400 µm) and chloral hydrate cleared seeds (9 DAP) (scale bars = 100 µm) respectively from a line expressing *ALE1* in the embryo in the *tws1-4* background (*pTWS1::ALE1 line#7*). H,I) Seeds from crosses of Col-0 pollen onto *line#7*. J,K) self-fertilized *tws1-4* seeds as a control L,M) Seeds from a cross of Col-0 pollen on a *tws1-4* pistil as a control. Results for three further independent transgenic lines are shown in Figs. S18 and S19. N) Complementation of *tws1-4* mutants by expression of TWS1 in the endosperm. Four independent lines were analysed. O) Model for embryonic cuticle integrity monitoring. Panel on left shows the wild-type situation prior to gap-filling (nascent cuticle), illustrating the diffusion and processing of TWS1 across the embryo-endosperm interface. Panel on right shows the wild-type situation when the cuticle is intact, spatially separating signalling components and thus the attenuating signalling.

Science
AAAS

Supplementary Materials for

A two-way molecular dialogue between embryo and endosperm required for seed development

Authors: N. M. Doll[1], S. Royek[2,†], S. Fujita[3,†, ‡], S. Okuda[4,†], A. Stintzi[2], T. Widiez[1], M. Hothorn[4], A. Schaller[2], N. Geldner[3], G. Ingram[1,*]

Correspondence to: Gwyneth.Ingram@ens-lyon.fr

This PDF file includes:

Materials and Methods
Figs. S1 to S23

Materials and Methods

Plant materials and lines used.

Except for peptide treatments, seeds were gas sterilized with chlorine (3Ml HCl (33%) in 150mL bleach) for 2 hours and then sown on Murashige and Skoog (MS) medium with 0,5% sucrose in sterile condition, stratified for 2 days at 4°C and grown for 7 days in long-day conditions (16h light, 21°C). Seedlings were then transferred to compost (Argile 10 (favorit)) and grown under long day conditions (16h light, 21°C). For staging the seeds, young flowers were marked every day for one week with cotton thread. For peptide treatments seeds were sterilized with 70 % ethanol for 10 min and briefly rinsed by 100 % ethanol, then dried under a sterile hood. Stratification was carried out at 4 ℃ for two days before incubation on half-strength solid Murashige-Skoog 1% agar medium. Plants were grown for 5 days under long day (18 h light /6 h dark) conditions at 22 ℃.

Mutant alleles used for loss-of-function analyses were *gso1-1* (*3*) for *GSO1* in all the experiments except for peptide activity assays on roots, for which the *sgn3-3* allele (SALK_043282) was used (*24*), *gso2-1* (*3*) for *GSO2*, *tpst-1* (*13*) and the weaker *sgn2-1* (*10*) for *TPST* and *ale1-4* (*5*) for *ALE1*. For *TWS1* we initially obtained the *tws1-1* and *tws1-2* alleles in the Wassilewskija (Ws) background (*14*). They were replaced by newly generated CRISPR alleles in the Col-0 background for all experiments (see below). The pCASP1::CASP1-GFP lines in Col-0 and *sgn3-3* background were described previously (*24*, *25*). The transgenic lines *pGSO1::GSO1::VENUS* (*21*) and *pPIN1::GFP* (*26*) were also used in this study.

Materials generated in this study

For *tpst* complementation, the cDNA of *TPST* was amplified using the *5'-ggggacaagtttgtacaaaaaagcaggctttatgcaaatgaactctgtttggaagc-3'* and *5'-ggggaccactttgtacaagaaagctgggtttcaaatcttaactttggaggttcttc-3'* primers with the Gateway extensions attB1-B2 and cloned by BP reaction into a *pDONR221* vector. Promoters *pRGP3* (*22*), *pPIN1* and *pRPS5a* (*21*) in *pDONR_P4_P1R* entry vectors were used. Triple LR reactions were performed with *TPST*, each of the three promoters, and a mock sequence with attP2-3 borders in a pK7m34GW plasmid using LR clonase II (Invitrogen).

The *pTWS1* promoter described by Fiume and co-workers *(14)*, was amplified with the primers *5'-ggggacaactttgtatagaaaagttgtttgaatgaaagttgtgttttgacaaa-3'* and *5'-ggggactgctttttgtacaaacttgtcttcttctctagagattgaggaagagg-3'* with attB4-B1R extensions and cloned by BP reaction in a *pDONR_P4_P1R* vector. For promoter reporter line, the *pTWS1* promoter, an *mCITRINE*-coding sequence with attP1-P2 borders and an *NLS-mCITRINE*-coding sequence with attP2-P3 borders were then cloned by triple LR reaction into a *pK7m34GW* destination vector.

The ORF of *ALE* was amplified by PCR with the primers 5'ggggacaagtttgtacaaaaaagcaggctttatggaaaccaatccaagaaaactaag-3' and 5'ggggaccactttgtacaagaaagctgggtttcaaatggttttaactgacaacggta-3' PCR products with the Gateway extensions attB1-B2 were cloned by BP reaction into a *pDONR221* vector.

The *GSO2* open reading frame was amplified from genomic DNA with the primer *5'-ggggacaagtttgtacaaaaaagcaggctttatgcagcaaaactctgttcttctt-3'* and *5'-ggggaccactttgtacaagaaagctgggtttttatcggtatcagtttgcatctc-3'* and cloned by BP reaction into *pDONR221*. For translational reporter lines, *GSO2*, *pGSO2* with *pDONR_P4_P1R* and a VENUS (yellow fluorescent protein) with attP2-3 borders were cloned in *pB7m34GW* vector by triple LR reaction.

The *TWS1, CIF 1 and CIF2* open reading frames were amplified by PCR using the primers *5'-ggggaccactttgtacaagaaagctgggtttccaccgtcttgggattgctg -3'* and *5'-ggggacaagtttgtacaaaaaagcaggctttatgaagacgtcaagctttgtcttcc -3'* for *TWS1*, *5'-ggggacaagtttgtacaaaaaagcaggctttatgggtatgtcaccattaacggtg-3'* and *5'-ggggaccactttgtacaagaaagctgggtttcaattgggtataagcttgaaagg-3'* for *CIF1* and 5'-*ggggacaagtttgtacaaaaaagcaggctttatgggtttgttgccattggtgaag* -3' and 5'-*ggggaccactttgtacaagaaagctgggtttcagttgggaataagcttgaaag* -3' for *CIF2*. PCR products with the Gateway extensions attB1-B2 were cloned by BP reaction into a *pDONR221* vector. *pTWS1::TWS1* was obtained by triple LR reaction with pTWS1 between the attP4-1R borders, TWS1 between the attP1-2 borders and a mock sequence between the attP2-3 borders. The *pTWS1::TWS1*$_{Y33->F}$ and *pTWS1::TWS1*$_{Y33->T}$ constructs were obtained by targeted mutagenesis from pTWS1::TWS1 in pB7m34GW using respectively the primer couples *5'-ggttggaggatttcaattttccagtggatcc -3'* and *5'- ctggaaaattgaaatcctccaaccccact -3'* and *5'-ggttggaggataccaattttccagtggatcc -3'* and *5'- ctggaaaattggtatcctccaaccccact -3'*. For complementation of *tws1-4* and *ale1-4* with TWS1 and CIF1 and CIF2 peptides in the endosperm, the *pRGP3* promoter *(22)* with attP4-P1R borders, the open reading frames of *TWS1*, *CIF1* and

CIF2 with attP1-P2 borders and a mock sequence with attP2-3 borders were cloned using triple LR reactions into a pK7m34GW destination vector.

For co-expression of ALE1 and TWS1 in tobacco, the *ALE1* cDNA was amplified with the primers *5'-ggggacaagtttgtacaaaaaagcaggctttatggaaaccaatccaagaaaactaag-3'* and *5'-ggggaccactttgtacaagaaagctgggtttcaaatggttttaactgacaacggta-3'* and the *TWS1* cDNA with the primers *5'-ggggaccactttgtacaagaaagctgggtttccaccgtcttgggatggctg-3'* and *5'-ggggacaagtttgtacaaaaaagcaggcttatatgaagacgtcaagctttgtcttcc-3'*.

For the generation of CRISPR alleles of *TWS1*, the method described by Wang and co-workers *(27)* for double guide assembly was applied. 2 vectors were generated, one for targeting the 5' end of the gene with 2 guides and the second for targeting the active (peptide encoding) domain with 2 guides. For targeting the 5' end of the gene, the primers *5'-atatatggtctcgattgtcaagctttgtcttcctttgtt-3'* and *5'-tgtcaagctttgtcttcctttgttttagagctagaaatagc-3'* were used for the first guide and *5'-aacaagcttctcactactagcttaatctcttagtcgactctac-3'* and *nd1_DT2-BsR 5'-attattggtctcgaaacaagcttctcactactagcttaa-3'* for the second guide. For targeting the active domain, the primers *5'-atatatggtctcgattggaggattacaattttccaggtt-3'* and *5'-tggaggattacaattttccaggttttagagctagaaatagc-3'* were used for the first guide and *5'-aacccaaccccactttcatttctaatctcttagtcgactctac-3'* and 5'-*attattggtctcgaaacccaaccccactttcatttctaa*-3' for the second guide.

The *cif1-2 cif2-2* double mutant was generated using the CRISPR-Cas9 technique described by Fauser and co-workers (*28*) with *5'-ttgggtataagcttgaaagg-3'* as a protospacer sequence. After establishing the *cif1-2 ci2-2* double homozygous mutant without the Cas9 construct, additional CRISPR-Cas9 constructs were transformed into *cif1-2 cif2-2* independently to generate *cif1-2 cif2-2 cif3-3* and *cif1-2 cif2-2 cif4-3* triple mutants using *5'-aacccaagcccggtttacgg -3'* and *5' ttgggaagaagtatttcacg-3'* as protospacer sequences respectively. These two triple mutants were crossed to obtain the *cif1-2 cif2-2 cif3-3 cif4-3* quadruple mutant.

Stable transformation of *Arabidopsis*

Plasmids generated for plant transformation were first transformed into the C58PMP90 Agrobacterial strain by electroporation at 2,2kV in a 1ml cuvette (Eurogenetec). Agrobacteria were then grown for 2h at 28°C in LB media without antibiotics before being spread on Petri dishes containing YEB solid media with rifampicin (50 µg.L-1), gentamicin (20 µg.L-1) for strain

selection, and spectinomycin (250 µg.L-1) for transgene selection. All plants were transformed using the floral-dip method described in *(29)*.

Toluidine blue permeability test

For assessing cuticle integrity, toluidine blue tests were performed, as described in *(30)*. For pictures of etiolated cotyledons, seedlings were stratified in the dark, exposed to a 4-6h light flash and then grown for 4 days in darkness before being stained for 2 min (unless indicated otherwise) in toluidine blue solution (0.05% w/v) with Tween 20 (0.1% v/v) and washed profusely in tap water. Pictures were taken either with a Leica MZ12 light microscope or with a VHX900F digital microscope (Keyence).

For toluidine blue quantification, 7 day old seedlings were stained as above. The aerial parts of ten seedlings were excised and placed in tubes containing 1 mL of ethanol 80%, for at least 2 hours in darkness, until all the toluidine blue and the chlorophyll had been extracted. Toluidine blue absorbance of the resulting solution was quantified as described in (*5*). Six repetitions were performed per condition.

Seed shape analysis

Percentages of misshapen seeds were counted on pictures taken with the Leica MZ12 light microscope, using the cell counter option of the ImageJ software. For each genotype, seeds from four plants were analysed, with at least 400 seeds per mother plant.

Peptide sequence alignments

Peptide sequence alignments were performed using the Probalign program (*31*).

Peptide activity in roots

For peptide treatment experiments, seeds were germinated on solid medium with or without indicated concentrations of peptides (Peptide Specialty Laboratories GmbH) and grown for 5 days.

Peptides used in this study

Sulfated CIF2 has already been described *(10)*. Non-sulfated TWS1 (DYNFPVDPTPTTKASIKPGPIEH), TWS1 (DY(sulfated)NFPVDPTPTTKASIKPGPIEH) and

TWS1+3AA Cter (DY(sulfated)NFPVDPTPTTKASIKPGPIEHGTP) peptides were synthetized by the Peptide Specialty Laboratories GmbH (Heidelberg).

Lignin staining using ClearSee

Lignin was co-visualized with CASP1-GFP using the ClearSee method (*32*, *33*). 5-day-old seedlings were fixed in 4% PFA solution in PBS pH6.9 for 1 hour without vacuum. After fixation, the seedlings were briefly rinsed with PBS solution twice. The samples were incubated in ClearSee solution overnight with shaking gently. The solution was then exchanged to 0.2 % fuchsin (Sigma) in ClearSee solution and gently shaken overnight. After removing the fuchsin solution, the samples were briefly rinsed with fresh ClearSee solution and incubated with another fresh solution for 30 min. The solution was again changed and the samples were incubated for at least one night.

CASP1-GFP and lignin were co-visualized using a Zeiss 880 microscope. Excitation and detecting windows were set as follows; GFP (488 nm, 500 - 550 nm) and Fuchsin (561 nm, 570 - 650 nm). For counting holes in Casparian strip domains, z-stack images of CASP1-GFP were gained around 10 cells after onset of CASP-GFP expression using a Leica SP8 microscope with 488 nm for excitation 500-550 nm for detection. The Images were projected as maximum projection and holes on the domains were counted. Image processing was performed by Fiji package of ImageJ. Statistical analysis was performed using R software (*34*) (https://www.r-project.org/). For multiple comparisons, one-way ANOVA was carried out followed by Tukey's tests.

Protein expression and purification

The constructs of SGN3 and GSO2 were described previously (*11*). For protein expression, *Trichoplusia ni* (strain Tnao38) (*35*) cells were infected with a multiplicity of infection (MOI) of 1 at a density of 2 x 10_6 cells ml_{-1} and incubated 26 h at 28 °C and 48h at 22 °C. The secreted protein was purified from the supernatant by Ni_{2+} (HisTrap Excel; GE healthcare; equibrated in 50 mM KP_i pH 7.6, 250mM NaCl, 1 mM 2-Mercaptoethanol) and StrepII (Strep-Tactin XT Superflow high affinity chromatography: IBA; equilibrated in 20 mM Tris pH 8.0, 250 mM NaCl, 1 mM EDTA) affinity chromatography. The tag was cleaved with TEV protease at 4 °C overnight and further purified by size-exclusion chromatography on a Superdex 200 increase 10/300 GL column (GE Healthcare), equilibrated in 20 mM sodium citrate pH 5.0, 250 mM NaCl.

Biotinylation of protein

Respective proteins (20 – 40 µM) were biotinylated with biotin ligase BirA (2 µM) (*36*) for 1hr at 25°C, in 200 µl of 25 mM Tris pH 8, 150 mM NaCl, 5 mM MgCl2, 2 mM 2-Mercaptoethanol, 0.15 mM Biotin, 2 mM ATP, followed by size-exclusion chromatography to purify biotinylated SGN3.

Grating – coupled interferometry

The Creoptix WAVE system (Creoptix AG, Switzerland) was used to perform GCI experiments. All experiments were performed on 4PCP WAVE chips (quasiplanar polycarboxylate surface; Creoptix, Switzerland). Chips were conditioned with borate buffer (100 mM sodium borate pH 9.0, 1 M NaCl; Xantec, Germany) and streptavidin (Sigma, Germany) was immobilized on the chip surface using standard amine-coupling; 7 min activation (1:1 mix of 400 mM *N*-(3-dimethylaminopropyl)-*N'*-ethylcarbodiimide hydrochloride and 100 mM *N*-hydroxysuccinimide (Xantec, Germany)), followed by injection of the streptavidin (50 µg.ml^{-1}) in 10 mM sodium acetate pH 5.0 (Sigma, Germany) until the desired density was reached, passivation of the surface (0.5 % BSA (Roche, Switzerland) in 10 mM sodium acetate pH 5.0) and final quenching with 1M ethanolamine pH 8.0 for 7 min (Xantec, Germany). Afterwards, biotinylated SGN3 or GSO2 (80 µg ml^{-1}) was captured on the chip surface. All kinetic analyses were performed at 25°C with a 1:2 dilution series starting from 500 nM for TWS1 sulfated peptides and CIF2 peptide or 10 µM for non-sulphated TWS1 in 20 mM citrate pH 5.0, 250 mM NaCl, 0.01 % Tween 20. Blank injections were used for double referencing and a dimethylsulfoxide (DMSO) calibration curve for bulk correction. Analysis and correction of the obtained data was performed using the Creoptix WAVE control software (correction applied: X and Y offset; DMSO calibration; double referencing). One-to-one binding models with bulk correction were used to fit the experiments for TWS peptides or a mass transport binding model for CIF2 peptide.

Co-expression of ALE1 and TWS1 in tobacco

For co-expression of ALE1 and TWS1 in tobacco, the *TWS1* cDNA was amplified with the primers *5'-ggggacaactttgtatagaaaagttgtttgaatgaaagttgtgttttgacaaa-3'* and *5'-ggggactgctttttgtacaaacttgtcttcttctctagagattgaggaagagg-3'* and cloned into *pDONR221* by BP reaction. Using this clone as the template, the *TWS1* ORF was amplified by PCR using oligonucleotide primers *5'-cctttatcgattccaccgtcttgggattgctgt-3'* and *5'-*

cctttatcgattccaccgtcttgggattgctgt-3'. The primers included XhoI and ClaI restriction sites to facilitate cloning of the PCR product in frame with the *sfGFP::(His)6* tag into *pART7*. The entire expression cassette comprising the *CaMV 35S* promoter, the *TWS1::sfGFP::(His)6* construct and the *OCS* terminator, was excised with NotI and inserted into the binary plant transformation vector *pART27* (*37*). Likewise, the *ALE1* cDNA was amplified with the primers *ALE1_F_attB* and *ALE1stop_R_attB* and cloned into *pDONR221*. Using this clone as the template, the 3'end of the *ALE1* cDNA was re-amplified by PCR to fuse six terminal His codons included in the primer (*1-3651-F; Ale1-2496R-Xba-His*). The 3'-end of the original *ALE1* cDNA was substituted with the PCR product to introduce the terminal *(His)6-tag*. The construct was cloned into *pART7* to result in *ALE1::(His)6-pART7*. As *ALE1-(His)6* was poorly expressed in *N. benthamiana*, we substituted the predicted N-terminal membrane anchor of ALE1 with the signal peptide of SBT4.13 (*9*). To this end, the 5'-end of *SBT4.13* ORF (including the signal peptide) and the N-terminal part of *ALE1* (lacking the signal peptide) were amplified by PCR (primer pairs *35S-P973-F / 48SP-ALE1_96R and 48SP-Ale1_96-F / ALE1-1846-R*, respectively). The two PCR products were joined by overlap PCR and cloned into *ALE1::(His)6-pART7* using an internal restriction site of *ALE1* (AflII), and a second site that is located in the upstream vector sequence (KpnI), resulting in *SP48::ALE1::(His)6-pART7*. The expression cassette including the *SP48::ALE1::(His)6* construct was then mobilized with NotI and cloned into *pART27*. All constructs were confirmed by Sanger sequencing (Macrogen; Amsterdam, The Netherlands).

ALE1::(His)6 and *TWS1::sfGFP::(His)6* expression constructs in *pART27* were transfected into A. tumefaciens *C58C1* for transient expression in N. benthamiana. *C58C1* strains containing the *SP48-ALE1-(His)6* or *TWS-sfGFP-(His)6* expression constructs in *pART27*, and *C58C1* containing the p19 suppressor of silencing were grown for two days on LB plates with appropriate antibiotics (rifampicin, tetracyclin and spectinomycin for *C58C1/pART27*; kanamycin instead of spectinomycin for *C58C1/p19*). Bacterial colonies were washed off the plates in 3 ml infiltration buffer (10 mM MES pH 5.6, 10 mM MgCl2, 0,15 mM acetosyringone). Bacteria were pelleted by centrifugation, the supernatant discarded and the pellet resuspended in 3 ml infiltration buffer. Bacteria were mixed at an OD600 ratio of 0.35 (*C58C1/pART27*) : 0.5 (*C58C1/p19*). A blunt syringe was used to infiltrate the bacterial suspension into leaves of six-week-old N. benthamiana plants. Three to five days after agro-infiltration, 12 leaf discs of 7 mm diameter were excised with a cork borer and flash frozen in in liquid nitrogen. A Tissue Lyser LT (Qiagen; Hilden, Germany) was used to shred the frozen leaf material to a fine powder. Total leaf protein

was extracted with 250 µl ice cold extraction buffer (100 mM NaCl, 50 mM Tris/HCl pH 7.5, supplemented with 0.5 % (v/v) Triton X-100, 10 mM β-mercaptoethanol and 10 µl/ml Protease-Inhibitor-Cocktail (Sigma-Aldrich; Steinheim, Germany), and the cell debris were removed by centrifugation (15000 x g, 4°C, 5 min). Protein concentration of the supernatant/total protein extract was determined using the Bradford assay with bovine serum albumin as the reference protein (BioRad).

33 µg total leaf protein was analysed by SDS-PAGE (15 %) followed by western blot using anti-(His)6 IgG (Dianova) (1:5000, overnight) as the primary, and rabbit-anti-mouse IgG peroxidase conjugate (2h, 1:10.000; Calbiochem) as the secondary antibodies (blocking solution: 1xTBS, 0,1% Tween, 1% BSA). Blots were developed using the SuperSignal® West Duran Extended Duration Substrate kit (Pierce/Thermo Fisher Scientific) and a Li-COR Odyssee imager (Li-COR; Bad Homburg, Germany) for chemiluminescence detection.

Analysis of TWS1 cleavage products by mass spectrometry

TWS1::sfGFP::(His)6 was co-expressed with *ALE1::(His)6* or the empty vector control in *N. benthamiana* leaves, and total leaf protein was extracted five days after agro-infiltration as described above (Triton X-100 and β-mercaptoethanol were omitted). 15 µL GFP-Trap®_A beads (Chromotek; Planegg-Martinsried, Germany) equilibrated in extraction buffer were added to 3.7 mg of total protein extract and incubated for 5 hours at 4°C on a rotating wheel. The beads were collected by centrifugation (2500 x g, 2 min, 4°C) and washed three times with 500 µl ice-cold extraction buffer. Proteins were eluted in 70 µl boiling 4x SDS sample buffer, separated by SDS-PAGE (15 %), and stained with Coomassie Brilliant Blue. Bands were excised and proteins were digested with proteomics-grade trypsin (Roche; Penzberg, Germany) in-gel according to (*38*). Digests were analyzed by nano-LC-ESI-MS/MS on an on an Ultimate 3000 RSLCnano system (Dionex, Thermo Fisher Scientific, Germany) coupled to a Q-Exactive HF-X mass spectrometer (Thermo Fisher Scientific) using an EASY-Nano Flex ion source (Thermo Fisher Scientific) in the Core Facility modul mass spectrometry (University of Hohenheim, Stuttgart). Peptides were separated by reversed phase HPLC (µ-precolumn C18 PepMap100, 300µm, 100Å, 5µm x 5mm (Thermo Fisher Scientific) followed by NanoEase M/Z HSS C18 T3, 1.8µm 100Å 75µm x 250mm analytical column (Waters; Eschborn, Germany)) at 35°C. Gradient elution was performed at a flow rate of 300nl/min 0.1% formic acid (solvent A) using a 30min gradient of 2% - 55% solvent

B (0.1% formic acid in 80% acetonitrile). The Q-Exactive HF-X was operated under the control of XCalibur software (version 4.1.31.9; Thermo Fisher Scientific). Survey spectra (m/z = 300-1800) were detected in the Orbitrap at a resolution of 60.000 at m/z = 200. Data-dependent MS/MS spectra were generated for the 20 most abundant peptide precursors using high energy collision dissociation (HCD) fragmentation at a resolution of 15000 with normalized collision energy of 27. Internal calibration was performed using lock-mass ions from ambient air as described in (*39*).

Cloning and site-directed mutagenesis of GST-TWS1 for expression in *E. coli*

Using the *TWS1* cDNA in *pDONR221* as the template, the *TWS1* ORF, excluding the start codon and signal peptide, was amplified by PCR with primers *5'-gggaaacccgggtctgaaatgaaagtggggttggagga-3'* and *5'-ttctttgaattcttatccaccgtcttgggattgctg-3'*. The primers included *Xma*I and *Eco*RI restriction sites to facilitate cloning of the PCR product in frame with the N-terminal *GST* tag into *pGEX-3X* (GE Healthcare). To introduce site-directed amino acid substitutions (P51A, E53A, H54A, G55L or T56A), the 3'-end of the cDNA was replaced by PCR products with corresponding codons exchanged using an internal *Hind*III restriction site of TWS1, and an *Eco*RI site in the multiple cloning site of the vector. For protein expression, *E. coli* BL21-CodonPlus (DE3)-RIL (Agilent Technologies) containing the respective *GST::TWS1* expression constructs were grown for one day in 25 ml LB with appropriate antibiotics (chloramphenicol, carbenicillin) at 37 °C, 220 rpm. This pre-culture was used to inoculate 300 ml LB with antibiotics to OD_{600} = 0.005. When OD_{600} reached 0.6, the culture was chilled to 30 °C. After 20 min, IPTG (1 mM) was added to induce protein expression. After 15 hours at 30 °C, 220 rpm, the bacterial cell pellet was harvested by centrifugation, resuspended in 30 ml lysis buffer (50 mM sodium phosphate pH 7.2, 150 mM NaCl, 10 µl/ml Protease-Inhibitor-Cocktail (Sigma-Aldrich; Steinheim, Germany), 1 spatula tip DNAseI (3200 U/mg), 5 mM PMSF, 10 mM benzamidine hydrochloride, 10 % glycerol), and lysed by sonication (4 x 30 s; Bandelin Electronic Sonicator; Berlin, Germany). The cell debris were removed by centrifugation and the supernatant added to 500 µl Glutathion HiCap beads (QIAGEN; Hilden, Germany) equilibrated in washing buffer (50 mM sodium phosphate pH 7.2, 150 mM NaCl, 1 mM DTT, 1 mM EDTA, 5 mM PMSF, 10 mM benzamidine hydrochloride). After 4 hours at 4 °C on a rotating wheal, the beads were transferred to a gravity-flow column, and washed three times with 12 mL washing buffer. GST-tagged proteins were eluted with six 500 µL aliquots of elution buffer (50 mM Tris pH 8.0, 0.4 M NaCl, 50 mM reduced glutathione, 0.1% Triton X-100, 1 mM DTT). The combined eluate was

concentrated to a final volume of 100 µl and the buffer exchanged to 50 mM sodium phosphate pH 8.0, 300 mM NaCl by ultrafiltration (Vivaspin, 10 k molecular weight cut-off (MWCO); Sartorius Stedim; Stonehouse, United Kingdom).

Purification of ALE1-6xHis

ALE1-$(His)_6$ was transiently expressed in *N. benthamiana* by agro-infiltration as described above. Five days after infiltration, 40 leaves were harvested and vacuum (70 mbar)-infiltrated with 50 mM sodium phosphate buffer, pH 7.0, 300 mM NaCl). For controls, the same amount of leaf material from empty vector-infiltrated plants was used and subjected to the same purification procedure. Apoplastic washes were collected by centrifugation (1500 x g, 10 min). The extract was cleared by centrifugation (20000 x g, 4°C) and the supernatant subjected to affinity chromatography on Ni-NTA agarose (QIAGEN; Hilden, Germany). 9.5 ml of the extract were incubated with 150 µL Ni-NTA beads for 1h at 4 °C on a rotating wheel. The suspension was transferred to a gravity flow column, washed 5 times with 7 ml assay buffer (50 mM sodium phosphate pH 8.0, 300 mM NaCl), and proteins were eluted in five 200 µL aliquots of 400 mM imidazole in assay buffer. Imidazol was removed and the eluate concentrated to a final volume of 95 µL by ultrafiltration (Vivaspin, 30k MWCO).

In vitro digestion of GST-TWS1 C-terminal mutants with ALE1

One µl of purified ALE1-$(His)_6$ or the mock purification was added to 1.5 µg GST-TWS1 and the P51A, E53A, H54A, G55L or T56A mutants in a total volume of 17 µL assay buffer. After 1 hr at room temperature, the reaction was stopped by adding SDS loading buffer, and the samples were analyzed by SDS-PAGE and Coomassie staining.

Transmission electron microscopy (TEM)

Seedlings collected 2 days after stratification were high-pressure frozen in a Leica EM-PACT-1 system. Seedlings were inserted into a flat copper carrier with hexadecene, fast-frozen, and cryosubstituted into the Leica AFS1 device. The freeze-substitution steps used were as follows: 54 hours at −90°C in acetone solution containing 0.2% glutaraldehyde (50% aqueous, EMS), 1% osmium tetroxide (EMS), and 0.1% uranyl acetate (EMS). The temperature was increased with steps of 2°C/hour before incubations at -60°C for 8 hours and -30°C for 8 hours. Three 10 minute washes in 100% acetone were performed at 4°C. Samples were then progressively embedded in

Spurr's resin (Spurr Low Viscosity Embedding Kit, Polysciences) as follows: 8 h in 25% resin in acetone, 24 h in 50% resin in acetone, 24 h in 75% resin in acetone and two times 24 h in 100% resin. Polymerization was performed for 18 h at 70°C.

70 nm sections were cut using a UC7 Leica ultramicrotome with a diamond knife and were imaged, without further contrasting, at 120 kV in a Phillips CM120 TEM with 2k x 2k Gatan Orius 200 ccd.

Auramine O staining

3-day-old seedlings were stained with a 0.5% solution of Auramine O (Sigma-Aldrich) in ClearSee solution as described in *(32).* After 12-16 hours of incubation in darkness, seedlings were washed in ClearSee twice quickly and then again for at least 1h before mounting in ClearSee solution. Confocal imaging was performed using a Zeiss LSM710 with 40X EC Plan Neofluar oil objective. Auramine O fluorescence was imaged with a 488nm diode laser excitation and detected with a 505-601nm PMT.

Confocal imaging

For observations by confocal microscopy, seeds were dissected from siliques and embryos from seeds with fine tweezers. Observations were carried out using a Zeiss LSM710 microscope with a 40X EC Plan Neofluor oil objective. Fluorescent proteins were excited at 514 nm and acquisition was performed between 520 and 558 nm and between 635 and 760 nm for the tissue autofluorescence.

Imaging of plants, seeds and seedlings

Dry seed images were taken with the Leica MZ12 light microscope. For clearing, developing seeds were dissected and cleared between slide and coverslip overnight in chloral hydrate solution (7/8 80% chloral hydrate (VWR chemical), 1/8 glycerol 87%% (Sigma)). Images were obtained using a Zeiss Axioimager 2 with transmitted light. Pictures of seedlings were taken with a VHX900F digital microscope (Keyence). Images of older plants were taken with a Cannon EOS 450D camera with a Sigma 50 mm f/2,8 DG Macro objective.

Quantitative gene expression analysis

Methods and primer sequences have all been described previously *(2)*

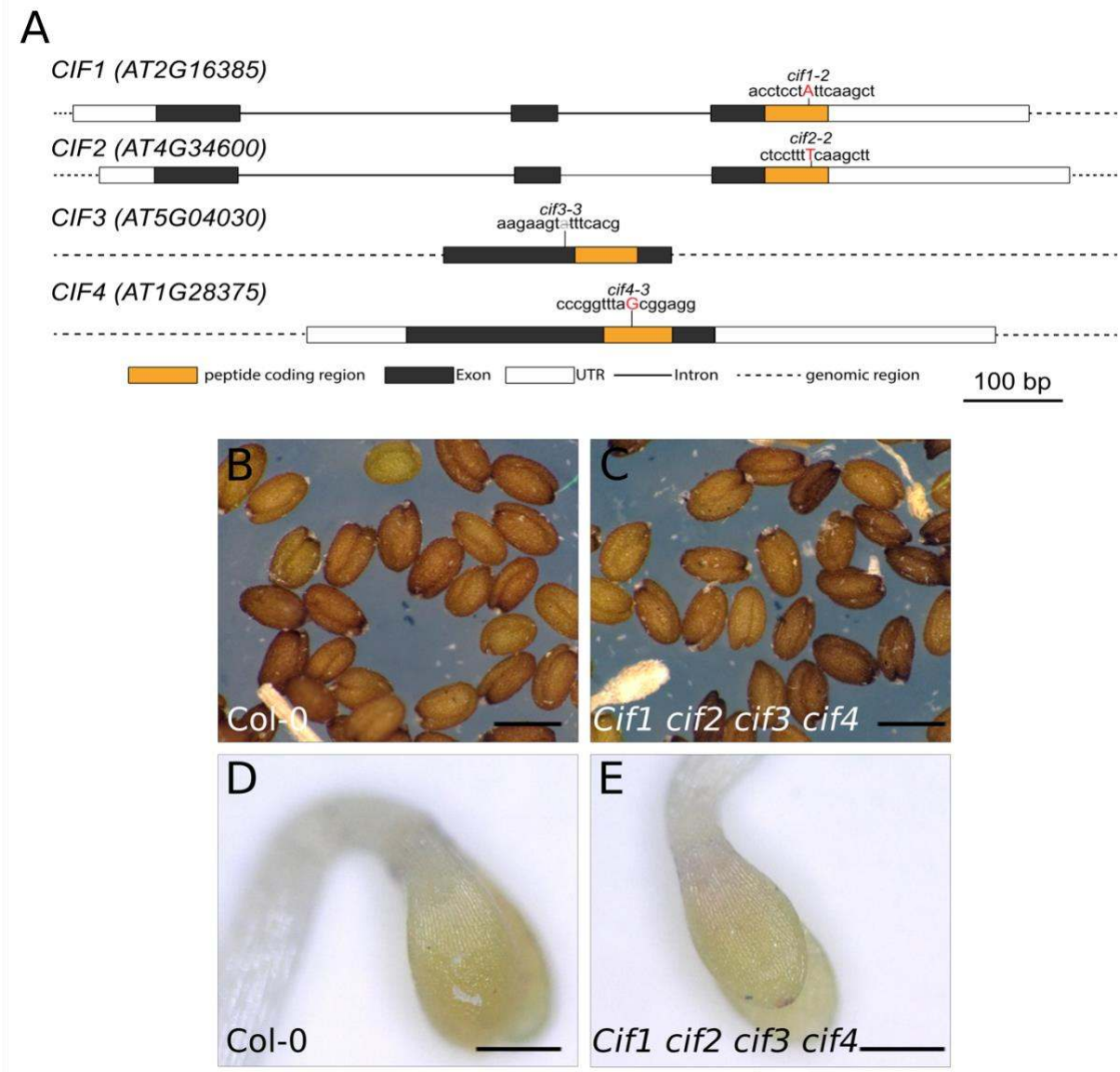

Fig. S1. The *cif1 cif2 cif3 cif4* quadruple mutant does not have defects in embryonic cuticle integrity. A) Mutations in the quadruple *cif* mutant. One base pair insertions (red letters in *cif1-2*, *cif2-2* and *cif4-3*) and and a one base pair deletion (grey letters with a line, *cif3-3*) are shown with the neighbouring sequences. B,C) Mature dry seeds B) Col-0 C) *cif1 cif2 cif3 cif4* quadruple mutant. D,E). Toluidine blue test on etiolated cotyledons. D) Col-0 E) *cif1 cif2 cif3 cif4* quadruple mutant. Scale bars in A,B = 200µm, in C,D = 400µm.

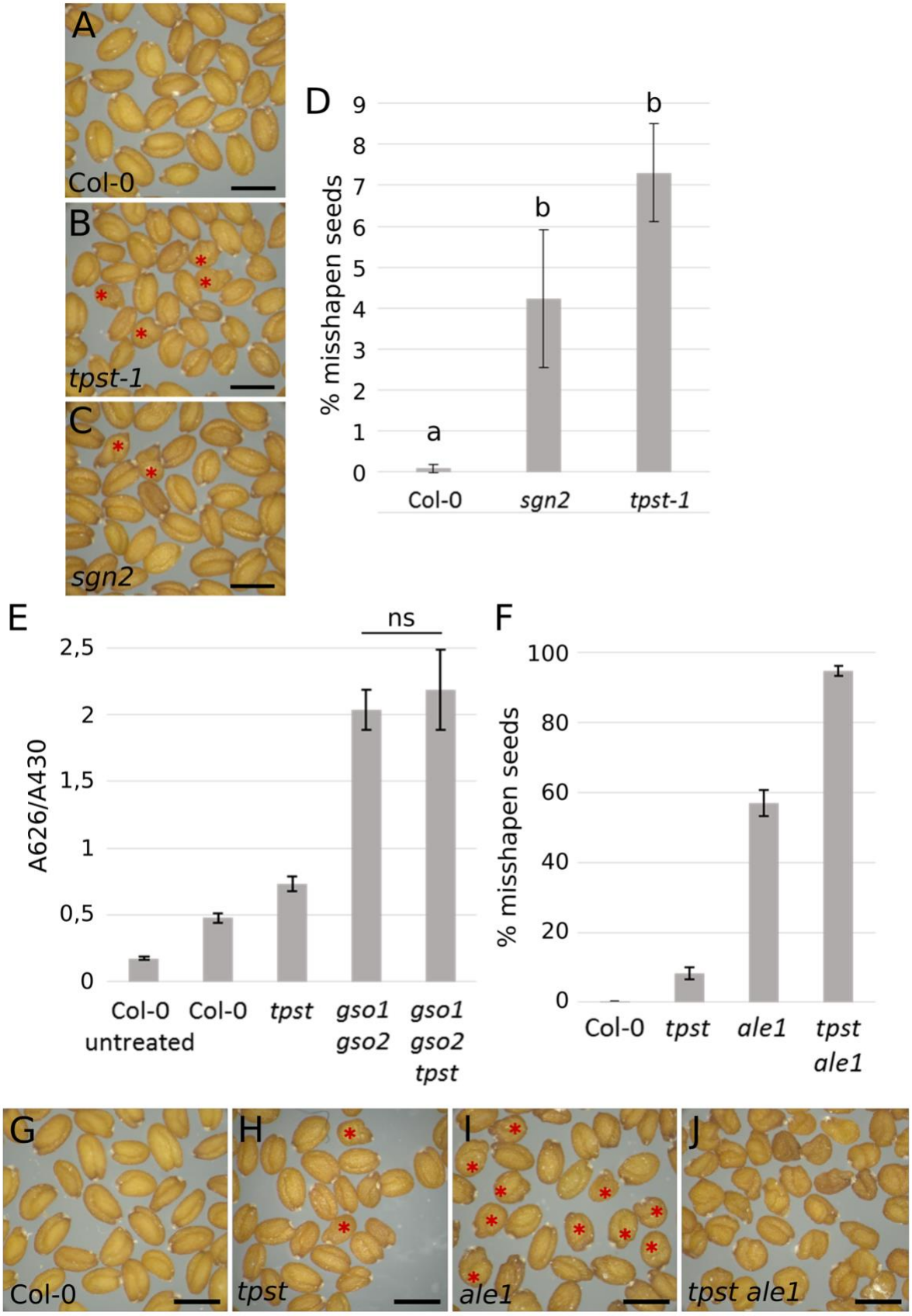
A
Col-0
B
tpst-1
C
sgn2
D
% misshapen seeds
9
8
7
6
5
4
3
2
1
0
a
b
b
Col-0
sgn2
tpst-1
E
ns
A626/A430
2,5
2
1,5
1
0,5
0
Col-0 untreated
Col-0
tpst
gso1 gso2
gso1 gso2 tpst
F
% misshapen seeds
100
80
60
40
20
0
Col-0
tpst
ale1
tpst ale1
G
Col-0
H
tpst
I
ale1
J
tpst ale1

Fig. S2. Further confirmation of genetic interactions of TPST with other cuticle integrity components. A-C) Seeds at maturity. A) Col-0, B) *tpst-1*, C) *sgn2*. Red stars indicate abnormal seeds. D) Percentage of misshapen seeds in *sgn2*, *tpst-1* and wild-type. N=4 (from independent mother plants). At least 300 seeds were counted per repetition. a, b = statistical differences with one-way ANOVA followed by a *post-hoc* Scheffé multiple comparison test ($P < 0,01$). E) Lack of additivity between *gso1 gso2* and *tpst.* Quantification of toluidine blue uptake into the aerial parts of young seedlings, normalized to chlorophyll content. N=6, ten seedlings per repetition. Ns = no statistical differences with one-way ANOVA ($P > 0,05$). F) Percentage of misshapen seeds in Col-0, *tpst-1, ale1-4, ale1-4 tpst-1*. N=4 (from independent mother plants). At least 300 seeds were counted per repetition. Mature seeds from G) Col-0, H) *tpst-1,* I) *ale1-4,* J) *ale1-4 tpst-1*. Red stars represent representative abnormal seeds in H) and I). Scale bars = 400µm.

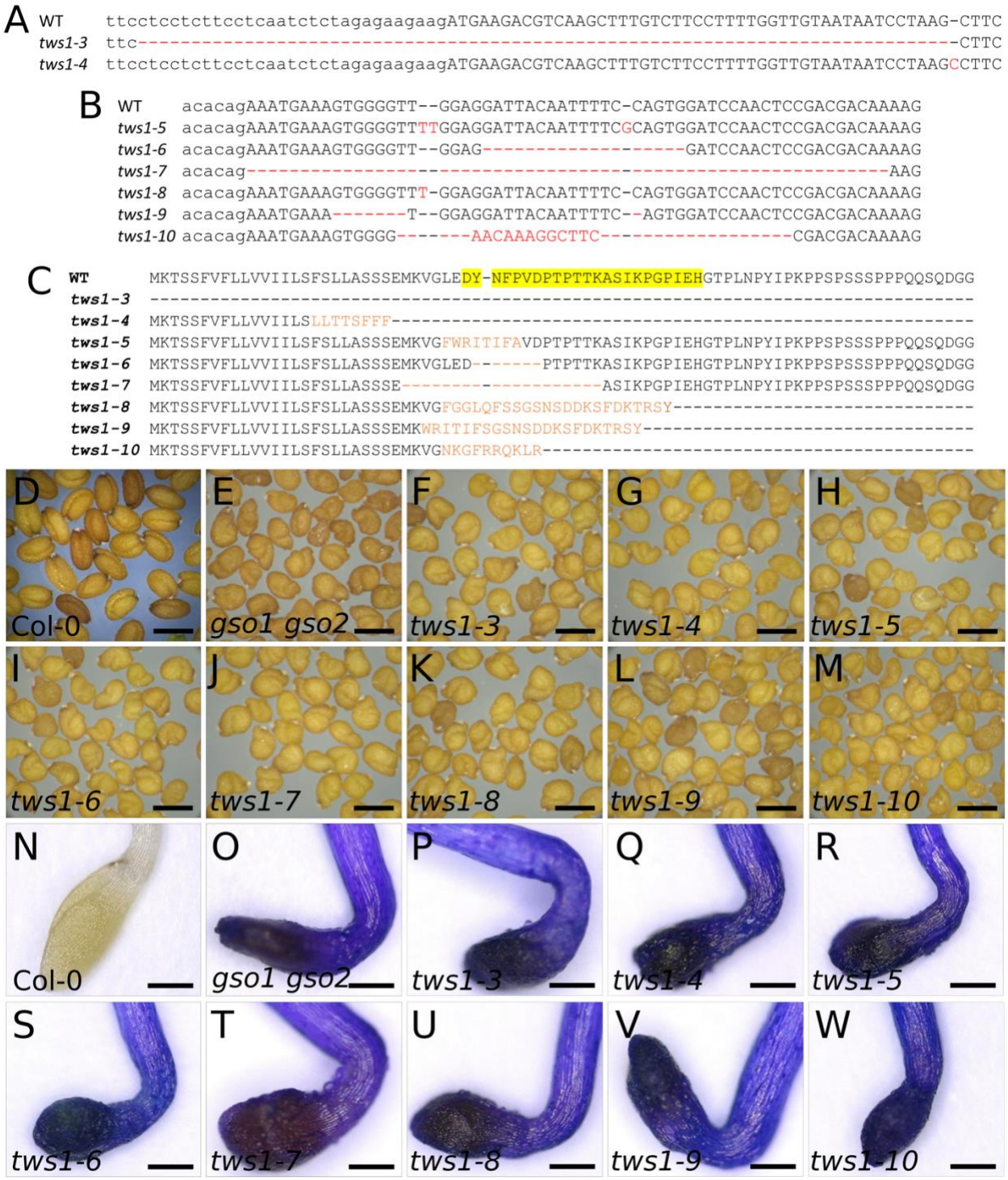

Fig. S3. CRISPR alleles of *TWS1* phenocopy *gso1 gso2* double mutants. A-B) DNA sequences of CRISPR alleles of *TWS1*. Mutations are labelled in red. C) Predicted protein sequences of the CRISPR alleles are shown in A-B. The mature TWS1 peptide is highlighted in yellow D-M) Photographs of mature seeds. Scale bars = 400µm D) Col-0, E*) gso1-1 gso2-1*, F) *tws1-3,* G) *tws1-*

4, H) *tws1-5*, I) *tws1-6*, J) *tws1-7*, K) *tws1-8*, L) *tws1-9*, M) *tws1-10*. N-W) Toluidine blue test on etiolated cotyledons. Scale bars = 200µm. N) Col-0, O*) gso1-1 gso2-1*, P) *tws1-3,* Q) *tws1-4*, R) *tws1-5*, S) *tws1-6*, T) *tws1-7*, U) *tws1-8*, V) *tws1-9*, W) *tws1-10*.

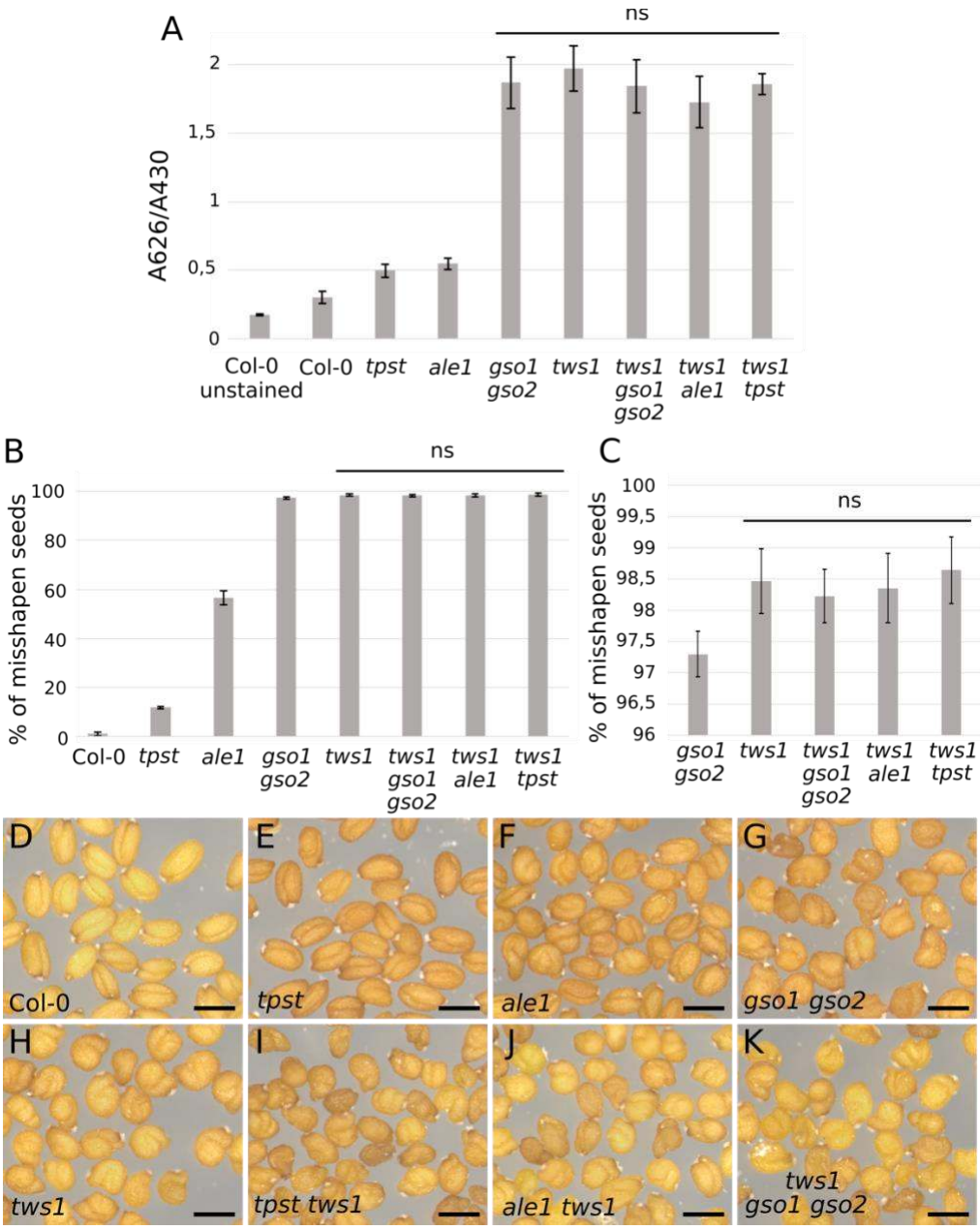

Fig. S4. ***tws1*** **shows no phenotypic additivity with GSO pathway mutants.** A) Quantification of toluidine blue uptake into the aerial parts of young seedlings, normalized to chlorophyll content. N=6, ten seedlings per repetition. Toluidine blue on multiple mutants of TWS1 and several GSO pathway components. B,C) Quantification of the number of misshapen seeds. For each lines, at least 400 seeds from 4 independent plants were analysed. Ns = no statistical differences with one-way ANOVA (P > 0,05) in A-C. Alleles used: *tpst-1, ale1-4, gso1-1, gso2-1, tws1-4*. C is a magnification of the upper portion of the last 5 samples shown in B. D-K)Photos of dry mature seeds. D) Col-0, E) *tpst-1*, F) *ale1-4*, G) *gso1-1 gso2-1*, H) *tws1-4*, I) *tpst-1 tws1-4*, J) *ale1-4 tws1-4*, K) *gso1-1 gso2-1 tws1-4*. Scale bars = 400µm of dry mature seeds.

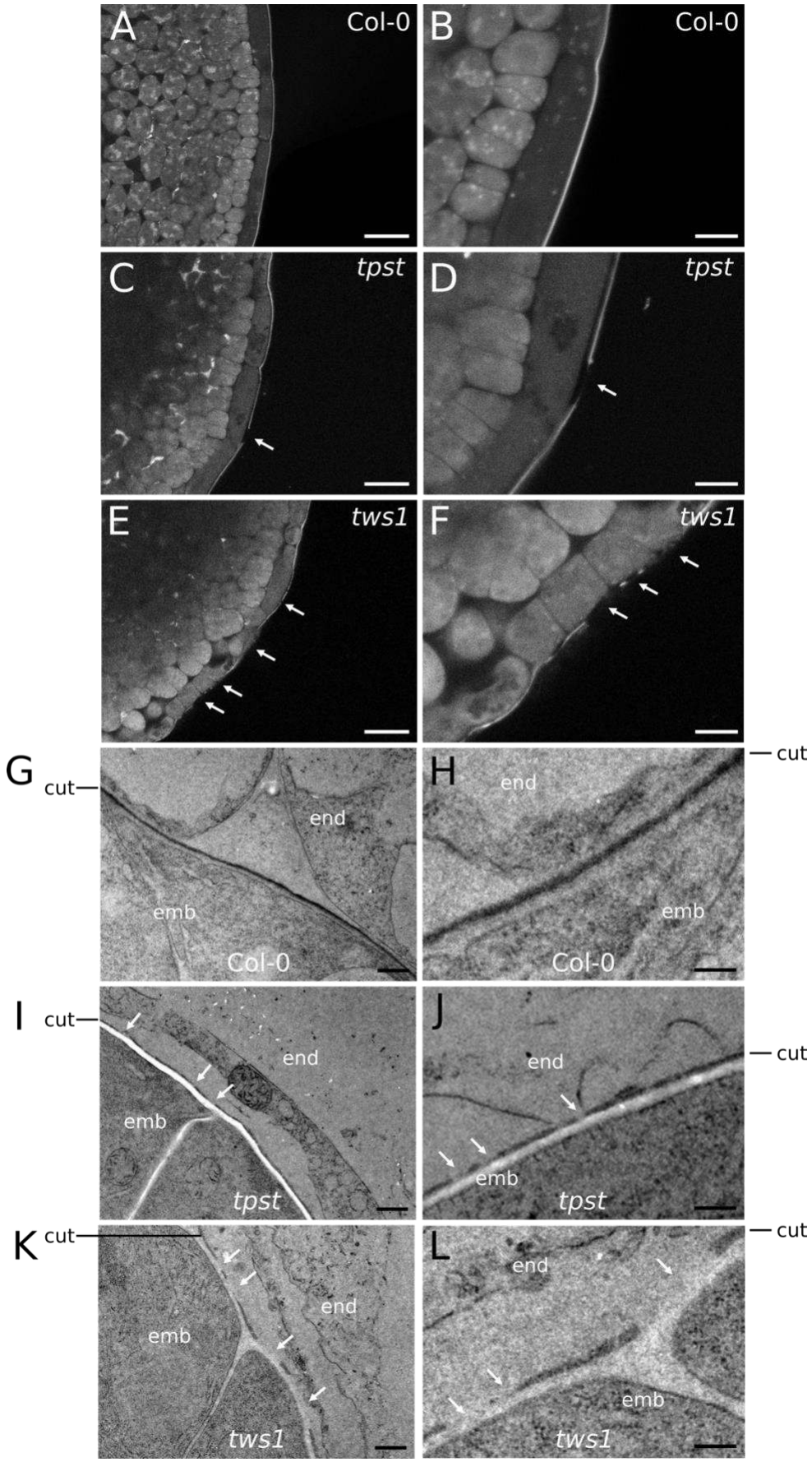
A
Col-0
B
Col-0
C
tpst
D
tpst
E
tws1
F
tws1
G
cut
end
emb
Col-0
H
cut
end
emb
Col-0
I
cut
end
emb
tpst
J
cut
end
emb
tpst
K
cut
end
emb
tws1
L
cut
end
emb
tws1

Fig. S5. *tws1* and *tpst-1* mutants have gaps in their embryonic and cotyledon cuticles. A-F) Auramine O staining of the cotyledon cuticle on seedlings 3 days after stratification, cleared using ClearSee (see materials and methods). A) Col-0, B) magnification of A, C) *tpst-1*, D) magnification of C, E) *tws1-4*, F) magnification of E. G-L) TEM pictures of embryo/endosperm interface at the heart stage. G,H) In Col-0, I,J) In *tpst-1*, K,L) in *tws1-4*. Arrows indicate the gaps in the cuticle. Scale bars = 10 µm in B,D,F, = 30 µm in A,C,E, = 500nm in G,I,K, = 200nm in H,J,L. emb = embryo, end = endosperm, cut = cuticle.

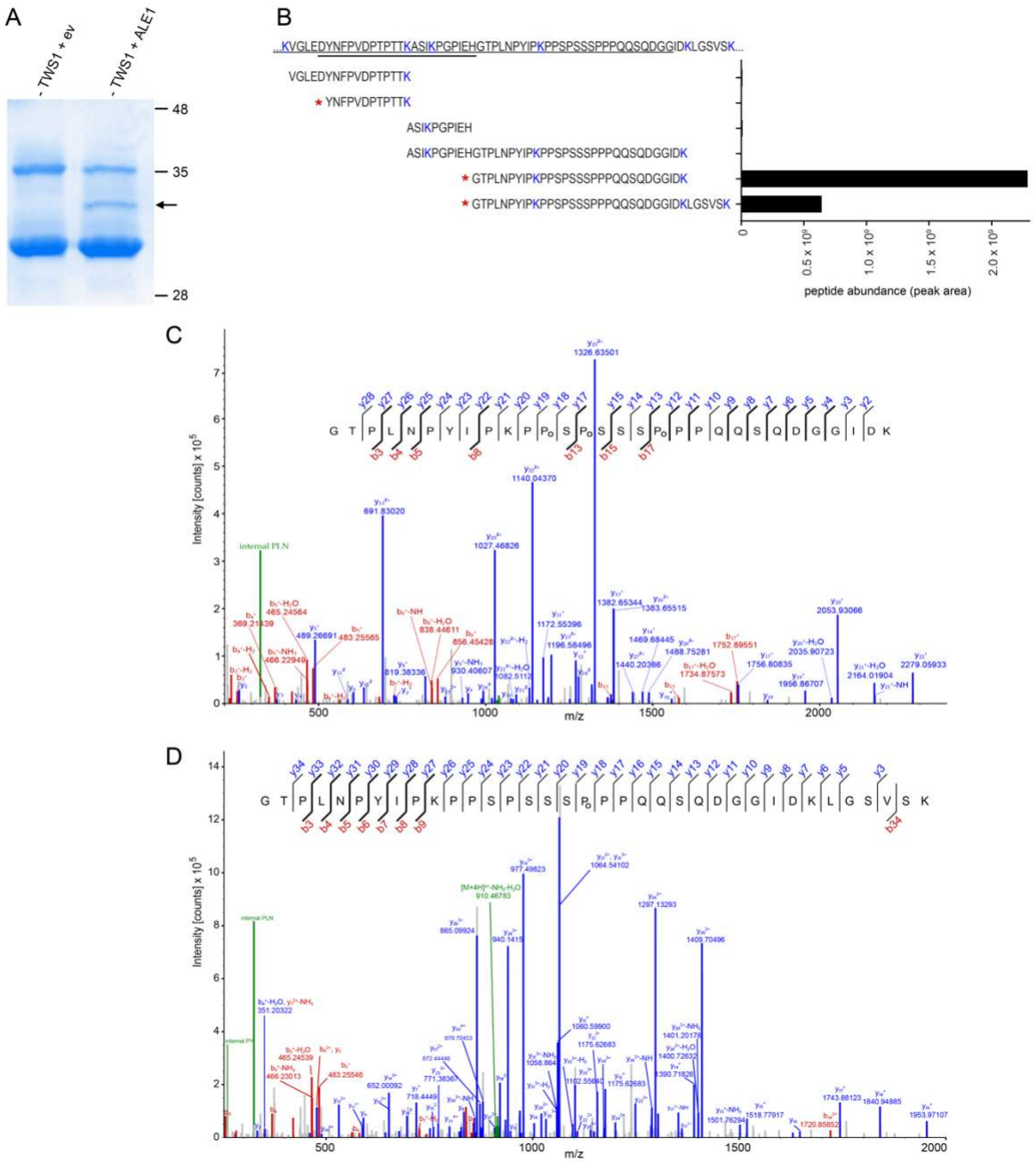

Fig. S6. ALE1 processes the C-terminus of TWS1. A) TWS1-GFP was co-expressed with ALE1-(His)6 or the empty vector control (ev) in *N. benthamiana* leaves. GFP-tagged proteins were pulled down with GFP-Trap and separated by SDS-PAGE. The ALE1-specific cleavage product (arrow) was cut out and digested in gel with trypsin. B) The sequence of proTWS1-GFP is shown on top (proTWS1 underlined; mature TWS1 double underlined; trypic cleavage sites highlighted as K). Peptides identified in the tryptic digest by MS analysis are shown below (non-tryptic cleavage events marked by red asterisks). Relative quantification of these peptides is shown in the bar graph (peak area in the extracted ion chromatogram). C and D) MS/MS analysis of the precursor ions of the two major peptides. Identity and sequence of the two peptides were confirmed by the almost complete y-ion series (blue) and additional ions from the b series (red). Both peptides

comprise the N-terminus of the ALE1-specific cleavage product (GTPL…) indicating processing by ALE1 of the H/G bond, marking the C-terminus of the mature TWS1 peptide.

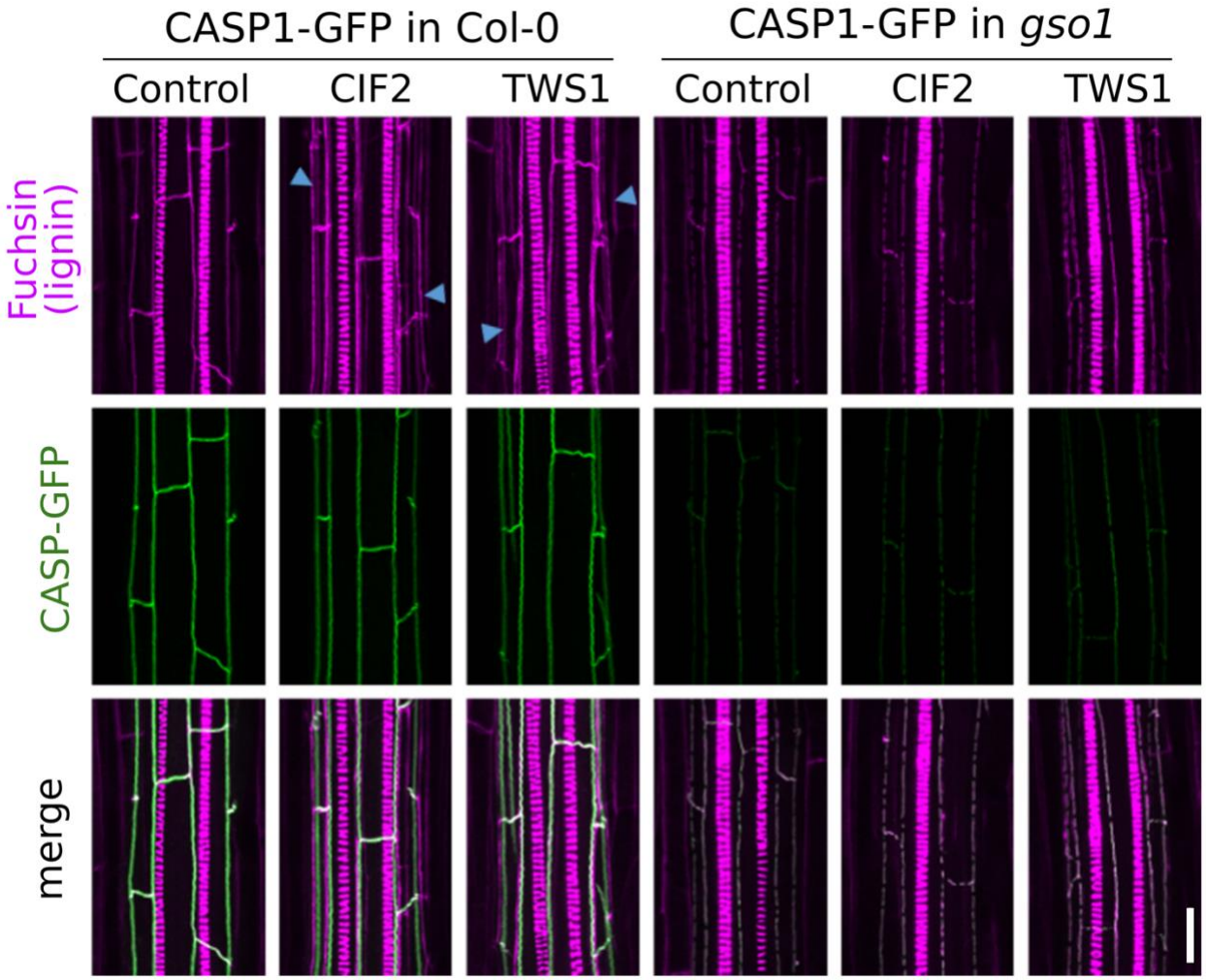

Fig. S7. TWS1 induces GSO1 dependent ectopic lignification in the root endodermis. Confocal images of root over-lignification following CIF2 or TWS1 treatment in Col-0 and in the *gso1 (sgn3-3)* background. Lignin stained with acid fuchsin in purple and CASP-GFP fusion protein, marking the Casparian strip domain in green. Scale bar = 20µm. Arrowheads indicate ectopic lignification. Figure 2A is a magnification of this figure.

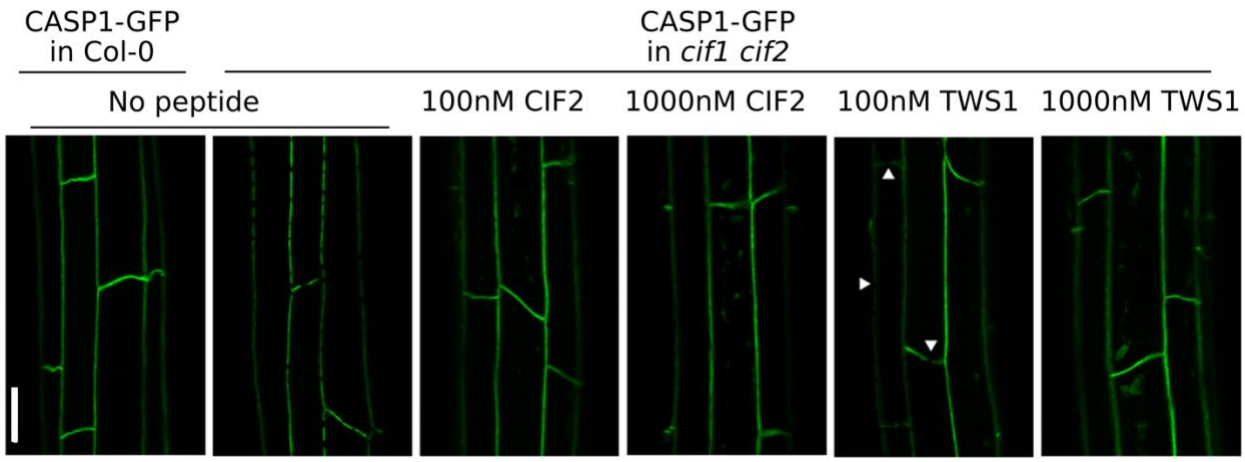

Fig. S8. TWS1 complements the Casparian strip integrity phenotype of the *cif1 cif2 mutant.* Confocal images of CASP-GFP localisation, marking the Casparian strip domain. Treatment of *cif1 cif2* roots with CIF2 and TWS1 peptides at different concentrations, in the same experiment as that shown in Figure 3C. Arrowheads indicate the holes in the CASP domain. Scale bar = 20µm.

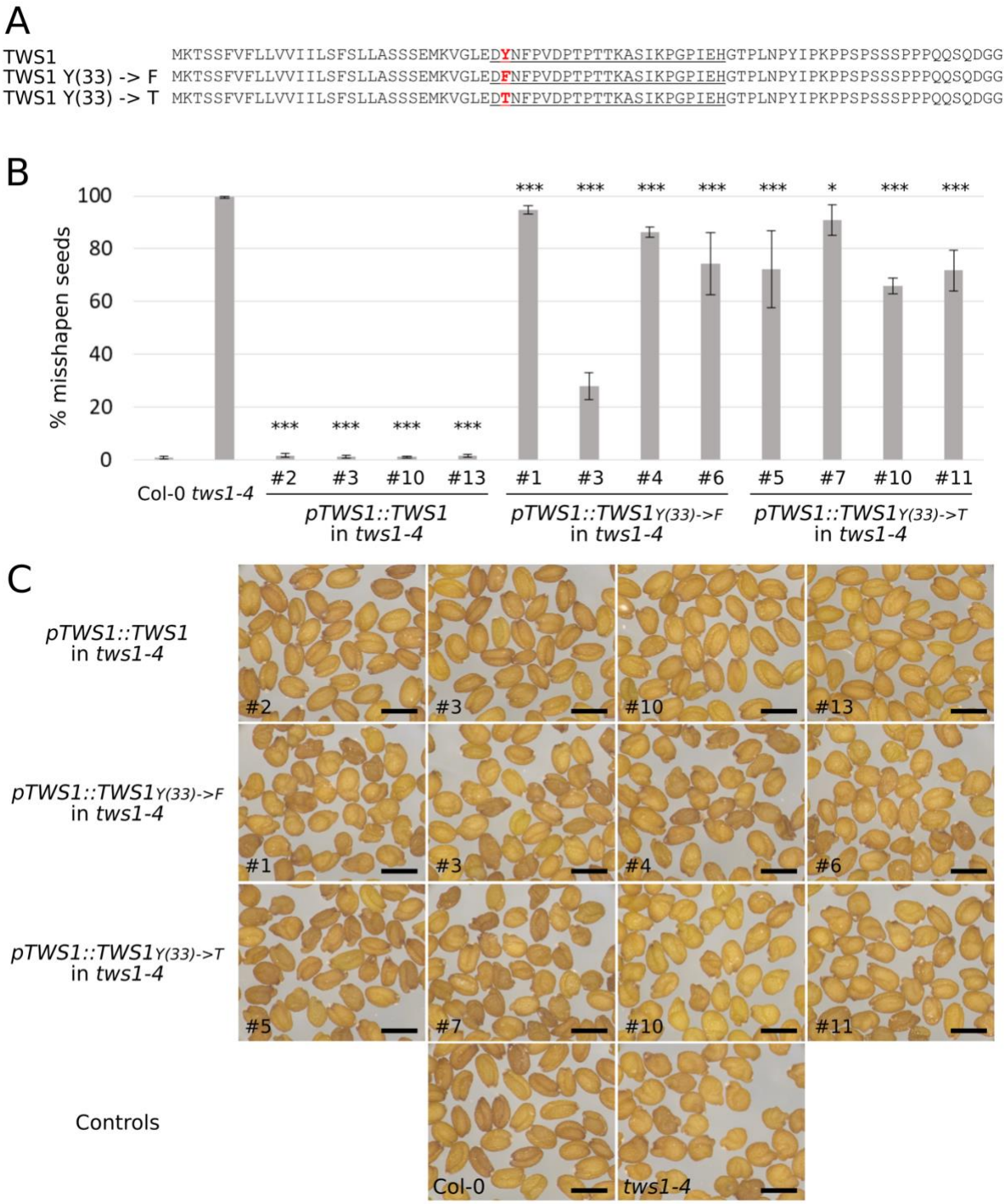

Fig. S9. Versions of TWS1 with substituted Y_{33} partially complement the *tws1* phenotype. A) Description of the TWS1 versions used for the complementation experiments. B) Quantification of the number of misshapen seeds in four independent lines for *pTWS1::TWS1* in *tws1-4*, *pTWS1::TWS1*$_{Y33\text{->}F}$ in *tws1-4* and *pTWS1::TWS1*$_{Y33\text{->}T}$ in *tws1-4* and controls Col-0 and *tws1-4*. For each line, at least 400 seeds from 4 independent plants were analysed. *** and * correspond to significant differences between *tws1-4* and each transgenic line using t-tests supported at $P < 0.01$ and $P < 0.05$ respectively. C) Images of seeds for four independent lines for *pTWS1::TWS1*

in *tws1-4*, *pTWS1::TWS1*$_{Y33->F}$ in *tws1-4* and *pTWS1::TWS1*$_{Y33->T}$ in *tws1-4* and controls Col-0 and *tws1-4.* Scale bars = 400µm.

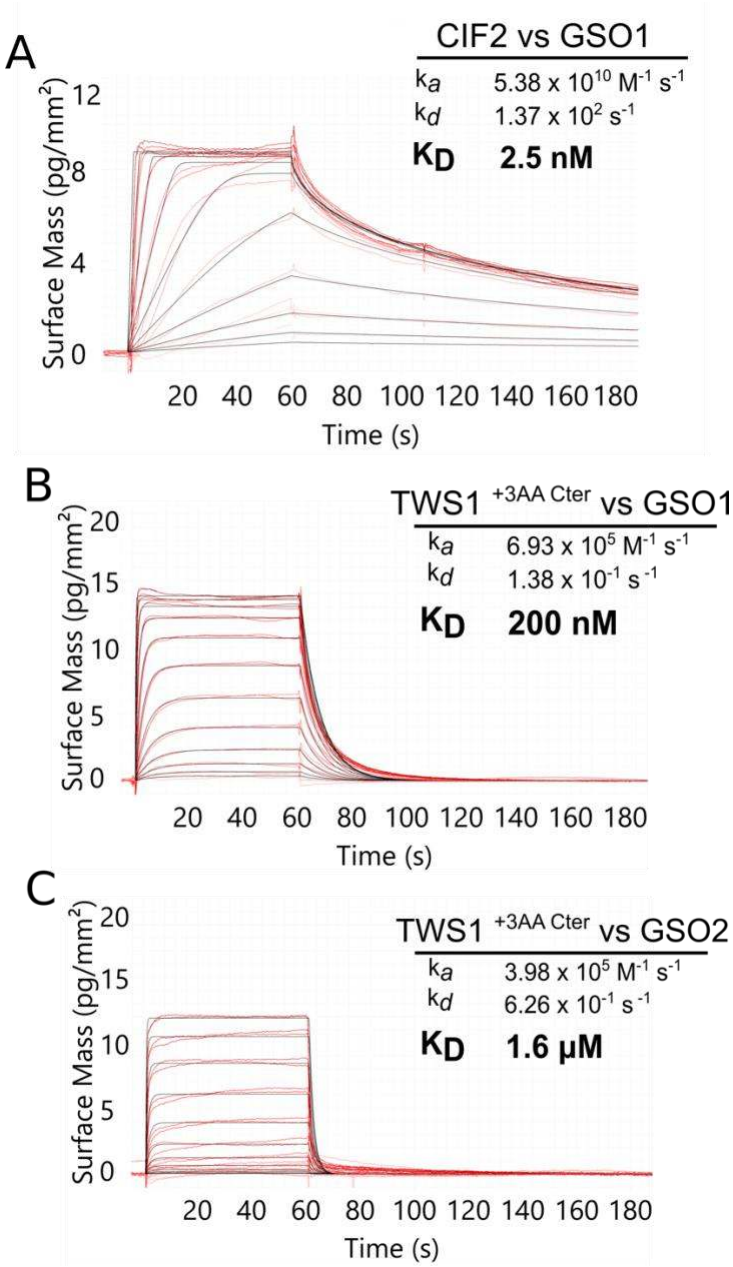

Fig. S10. Supplemental grating-coupled interferometry assays. Grating-coupled interferometry (GCI)-derived binding kinetics are shown. A) Shows is sensorgram with raw data in red and respective fit in black on the GSO1 extra-cellular domain in the presence of the sulfated CIF2 peptide. B) As for A) but showing binding kinetics of the sulfated TWS1 peptide including a 3AA C-terminal extension. C) As for B) but showing binding to the GSO2 extracellular domain. k_a, association rate constant; k_d, dissociation rate constant; K_D, dissociation constant.

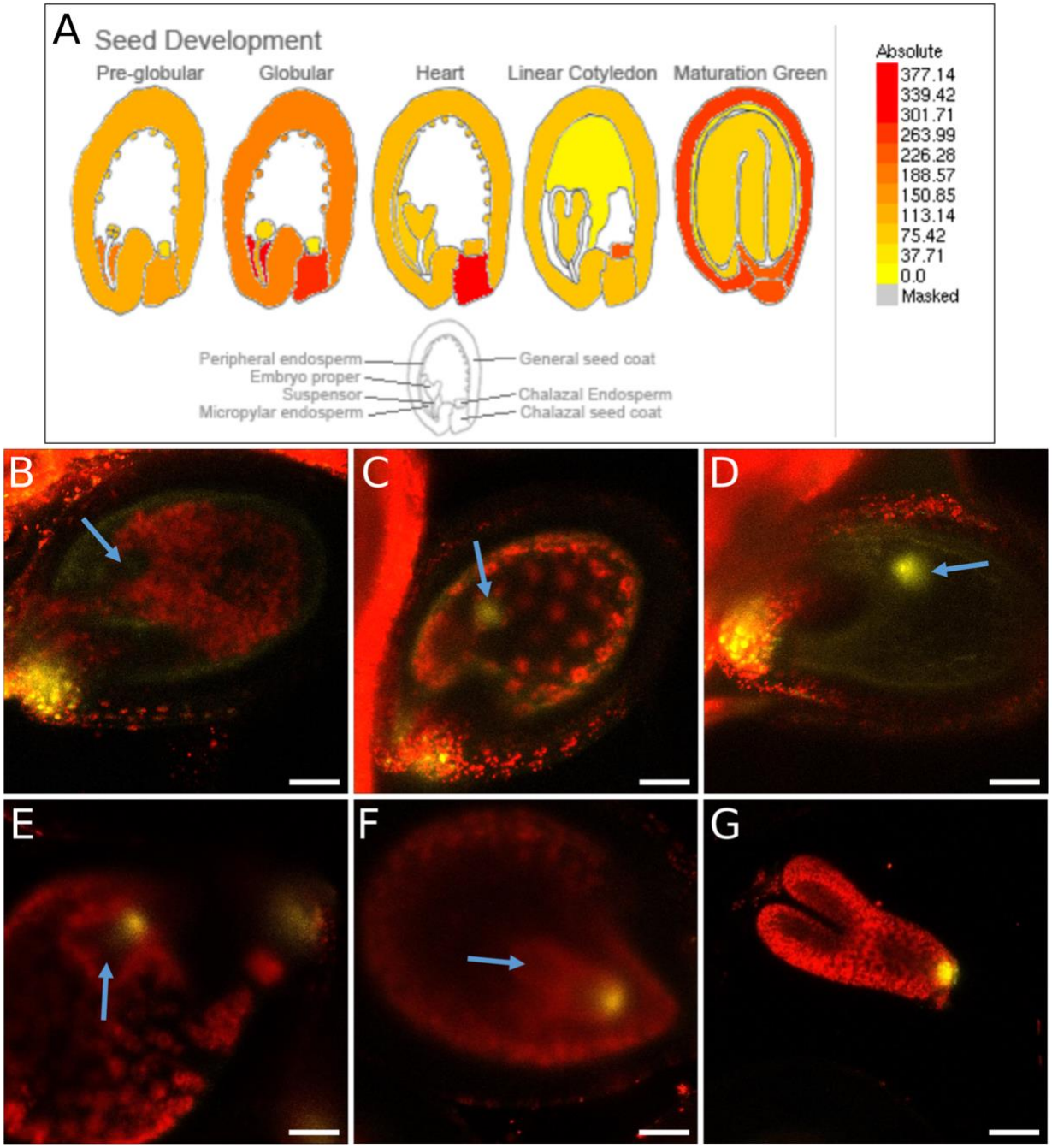

Fig. S11. *TPST* is expressed in all seed tissues including the embryo. A) *In silico* expression data for *TPST* in developing seeds. Z projections of confocal images from lines containing *pTPST::mCitrine::NLS-mCitrine* in seed. mCitrine signal is shown in yellow and autofluorescence in red B) Seed at pre-globular stage, C) Seed at early globular stage, D) Seed at late globular stage, E) Seed at heart stage, F) Seed at torpedo stage. G) Dissected embryo at torpedo stage. Scale bars = 50µm, arrows indicate the embryo proper.

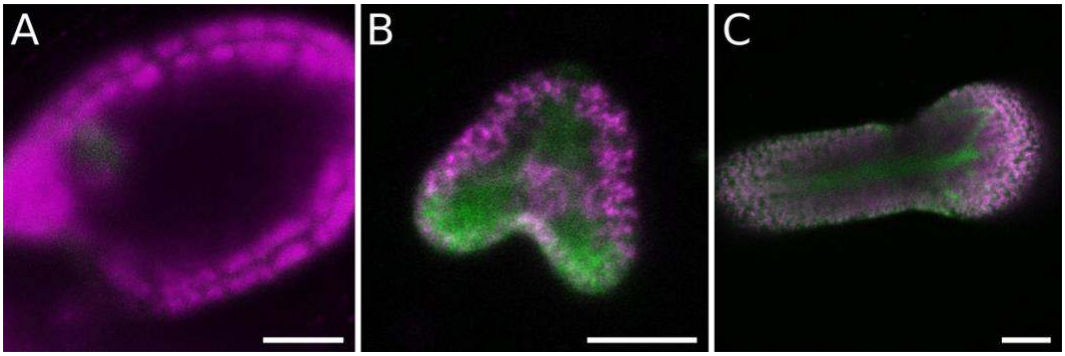

Fig. S12. *pPIN1* drives embryo specific expression during early seed development. Z projection of confocal images of *pPIN1::GFP* reporter line, signal in green, autofluorescence in magenta. A) Whole seed at globular stage, B) embryo at heart stage, C) Embryo at torpedo stage. Scale bars = 50µm.

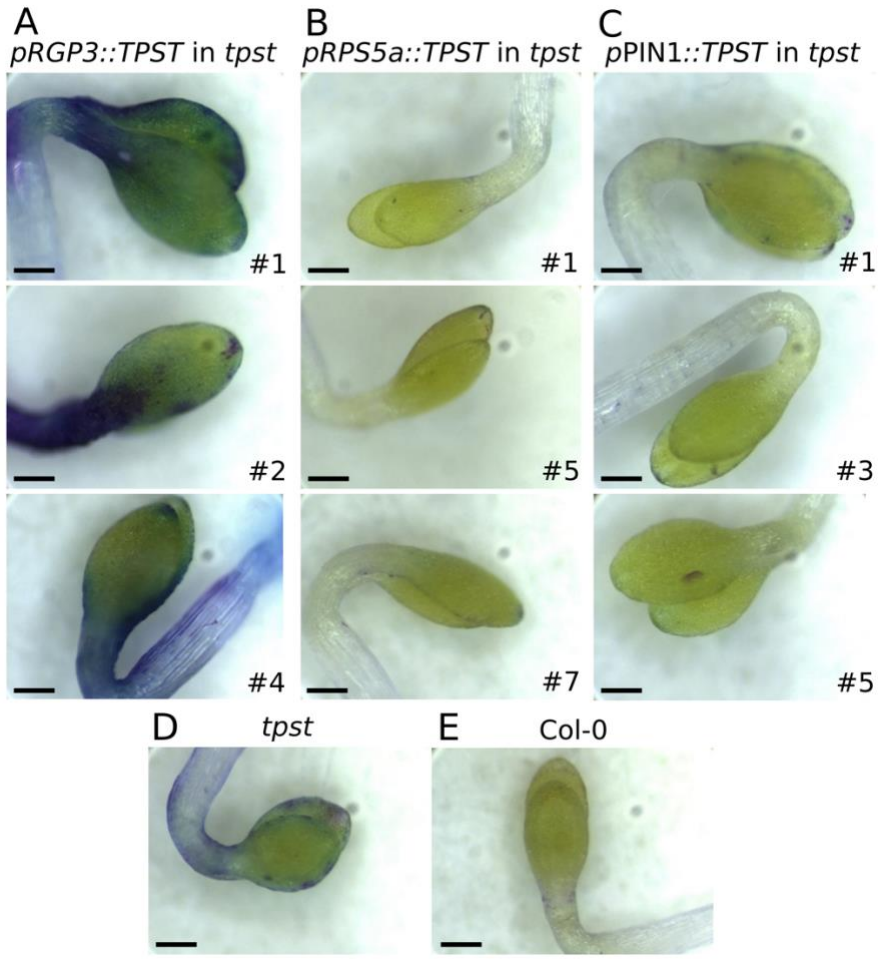

Fig. S13. TPST is necessary in the embryo, but not the endosperm for the formation of an intact embryonic cuticle. A) Three independent lines containing *pRGP3::TPST* in the *tpst-1* background (expressing *TPST* in the endosperm). B) Three independent lines containing *pRPS5a::TPST* in the *tpst-1* background (expressing TPST ubiquitously). C) Three independent lines containing *pPIN1::TPST* in the *tpst-1* background, (expressing *TPST* in the embryo). D) *tpst-1* E) Col-0. Scale bars = 200µm.

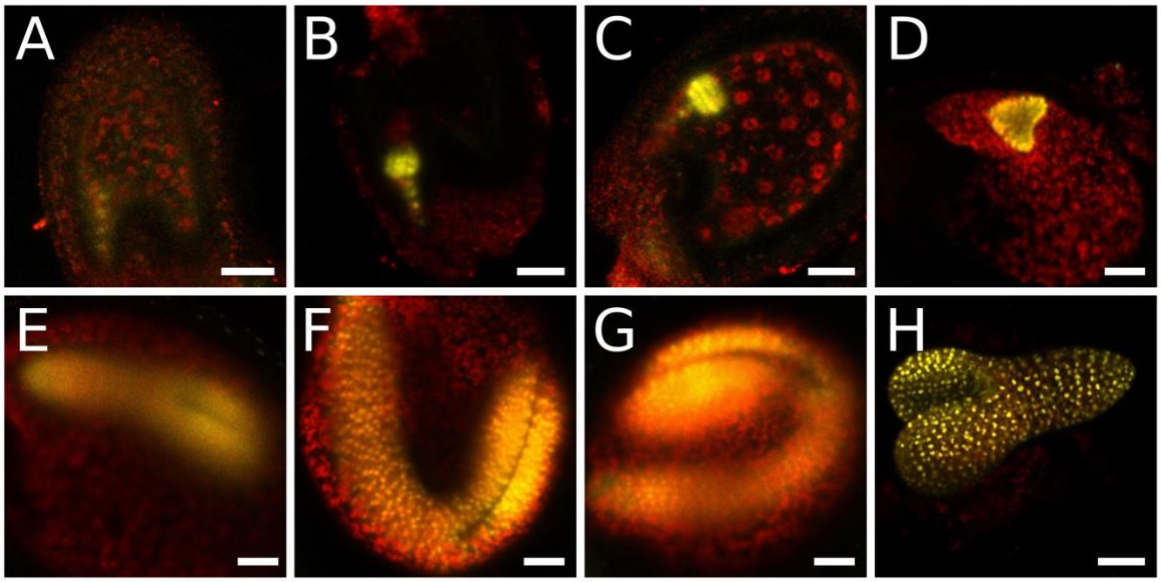

Fig. S14. *TWS1* shows strong embryo specific expression in seeds from the pre-globular stage onwards. Z projections of confocal images of *pTWS1::mCitrine::NLS-mCitrine* reporter lines, signal in yellow, autofluorescence in red. A-G) in developing seeds A) pre-globular stage, B) early globular stage, C) late globular stage, D) heart stage, E) linear cotyledon stage F) bent-cotyledon stage, G) mature seed, H) dissected embryo at torpedo stage. Scale bars = 50µm.

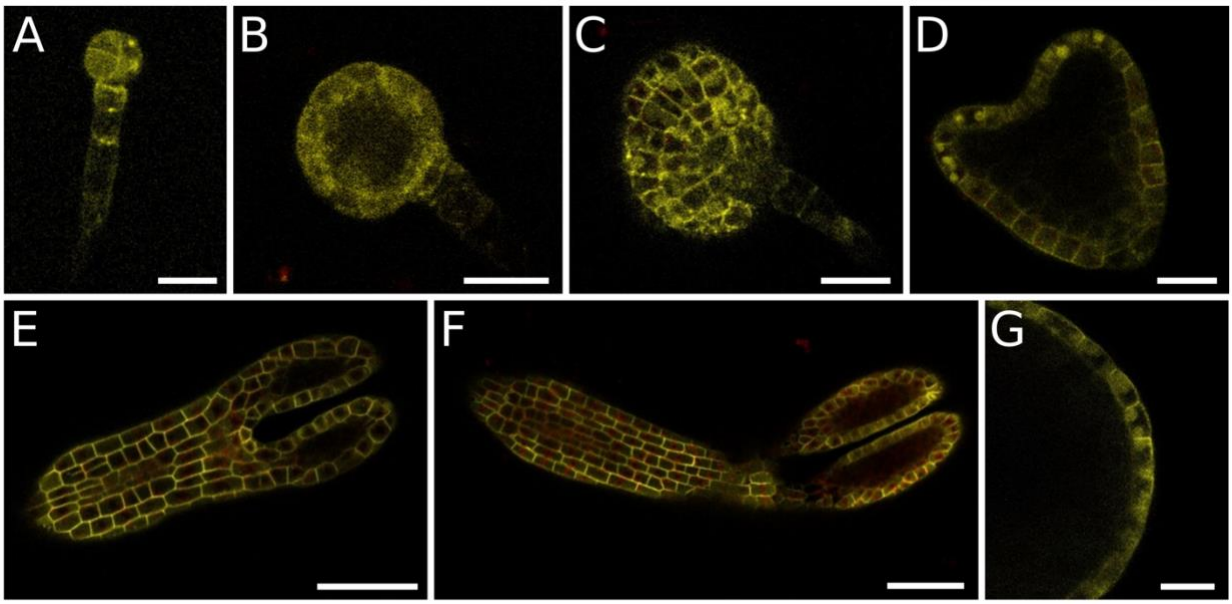

Fig. S15. GSO1 localises to the plasma membrane and internal compartments of the embryonic epidermis from the pre-globular stage onwards. Z projection of confocal images of embryos from transgenic lines containing the *pGSO1::GSO1::VENUS* construct. YFP signal in yellow and tissue autofluorescence in red. A) octant stage, B) globular stage, C) transition stage, D) heart stage, E) torpedo stage, F) bent-cotyledon stage, G) zoom on a cotyledon at bent-cotyledons stage. Scale bars = 10µm in I and K; 20µm in A, B, C, D and G; 50µm in E, F, H and J.

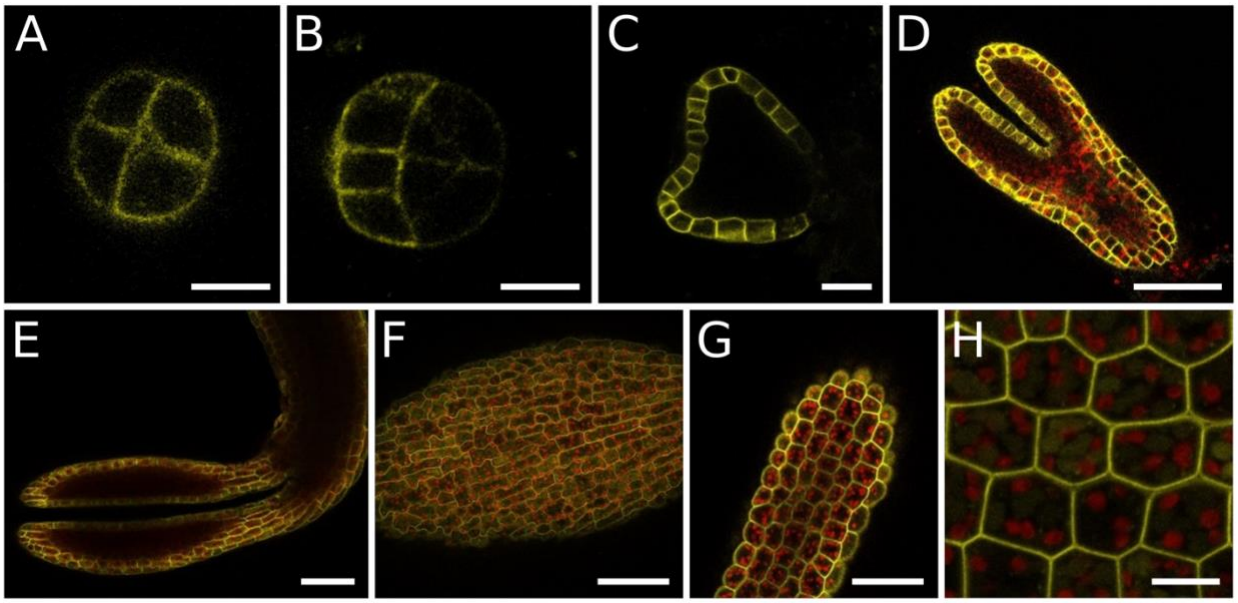

Fig. S16. GSO2 localises to the plasma membrane and internal compartments of the embryonic epidermis from the pre-globular stage onwards. Z projection of confocal images of embryos from transgenic lines containing the *pGSO2::GSO2::VENUS* construct. YFP signal is shown in yellow and tissue autofluorescence in red. A) Octant stage, B) globular stage, C) heart stage, D) torpedo stage, E) bent-cotyledon stage, F) cotyledon surface at mature stage, G) embryonic axis surface at mature stage, H) magnification of G. Scale bars = 10µm in A, B and H ; 20µm in C, 50µm in D, E, F and G.

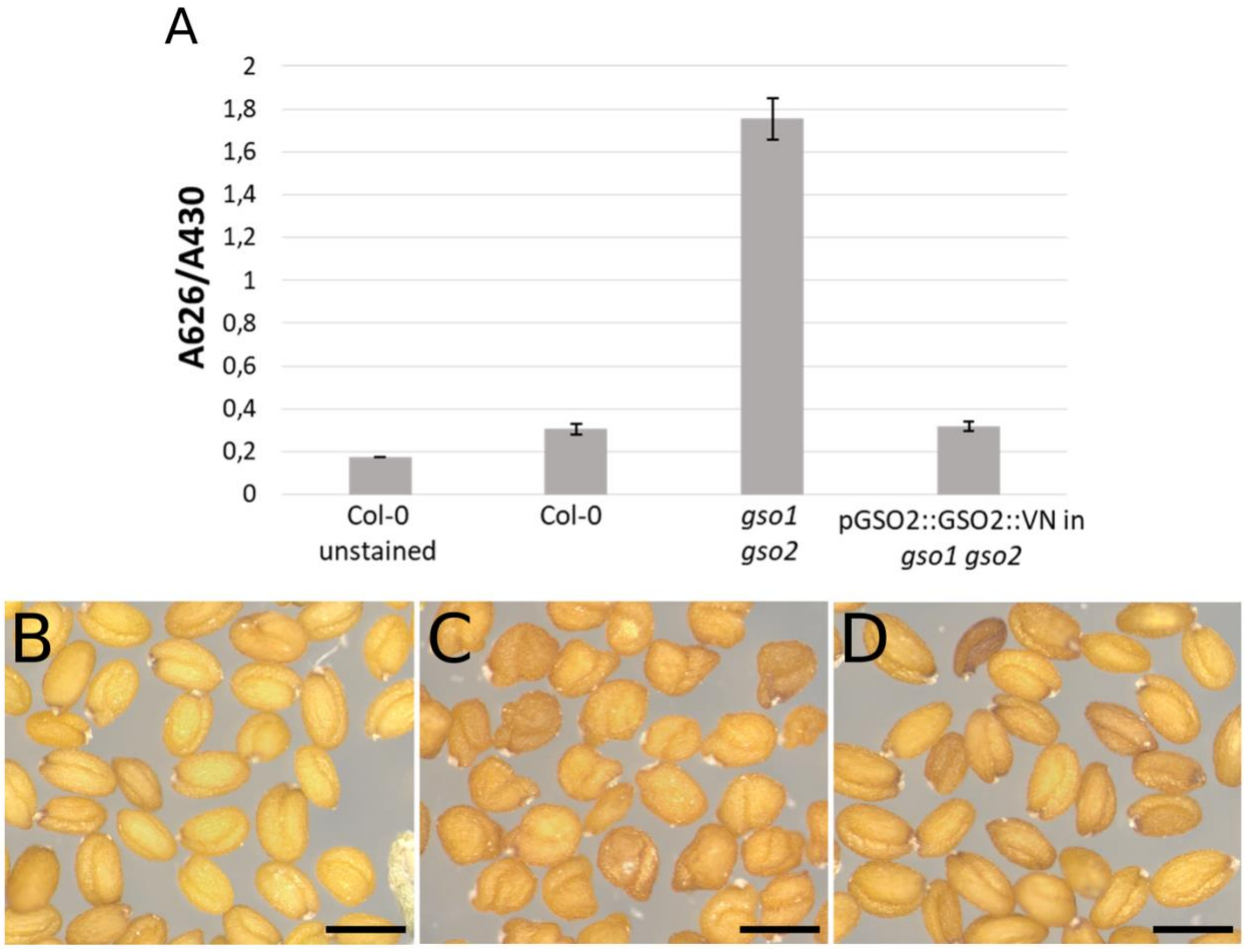

Fig. S17. *pGSO2:GSO2*::*VENUS* complements the seed phenotype of the *gso1 gso2* double mutant. A) Quantification of toluidine blue uptake into the aerial parts of young seedlings, normalized to chlorophyll content, on *pGSO2::GSO2::VENUS* in *gso1-1 gso2-1* compared to *gso1-1 gso2-1* and Col-0. N=6, ten seedlings per repetition. B-D) Photos of dry seeds at maturity. Scale bars = 400µm B) Col-0, C) *gso1-1 gso2-2*, D) *pGSO2::GSO2::VENUS* in *gso1-1 gso2-1*.

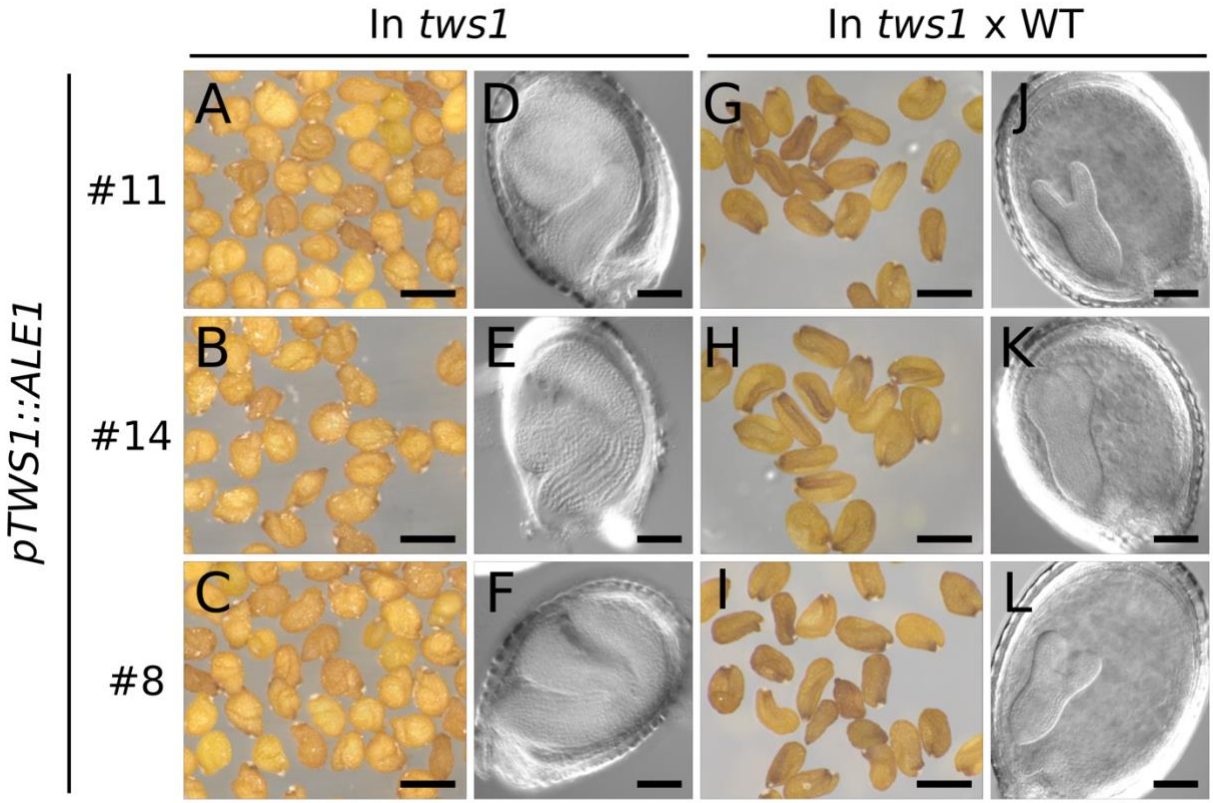

Fig. S18. Co-expression of ALE1 and TWS1 in the embryo induces severe developmental phenotypes in the embryo. A-C,G-I) Photos of seeds at maturity, Scale bars = 400µm. A-C) Seeds from three independent transgenic lines expressing *ALE1* in the embryo (*pTWS1::ALE1*) in the *tws1-4* background. G-I) Seeds from crosses of Col-0 pollen onto three independent lines expressing *ALE1* in the embryo (*pTWS1::ALE1*) in the *tws1-4* background. D-F,J-L) Chloral hydrate clearing on 9DAP (Days After Pollination) seeds. Scale bars = 100µm. D-F) Seed from three independent transgenic lines expressing *ALE1* in the embryo (*pTWS1::ALE1*) in the *tws1-4* background. J-L) Seed from crosses of Col-0 pollen onto three independent lines expressing *ALE1* in the embryo (*pTWS1::ALE1*) in the *tws1-4* background.

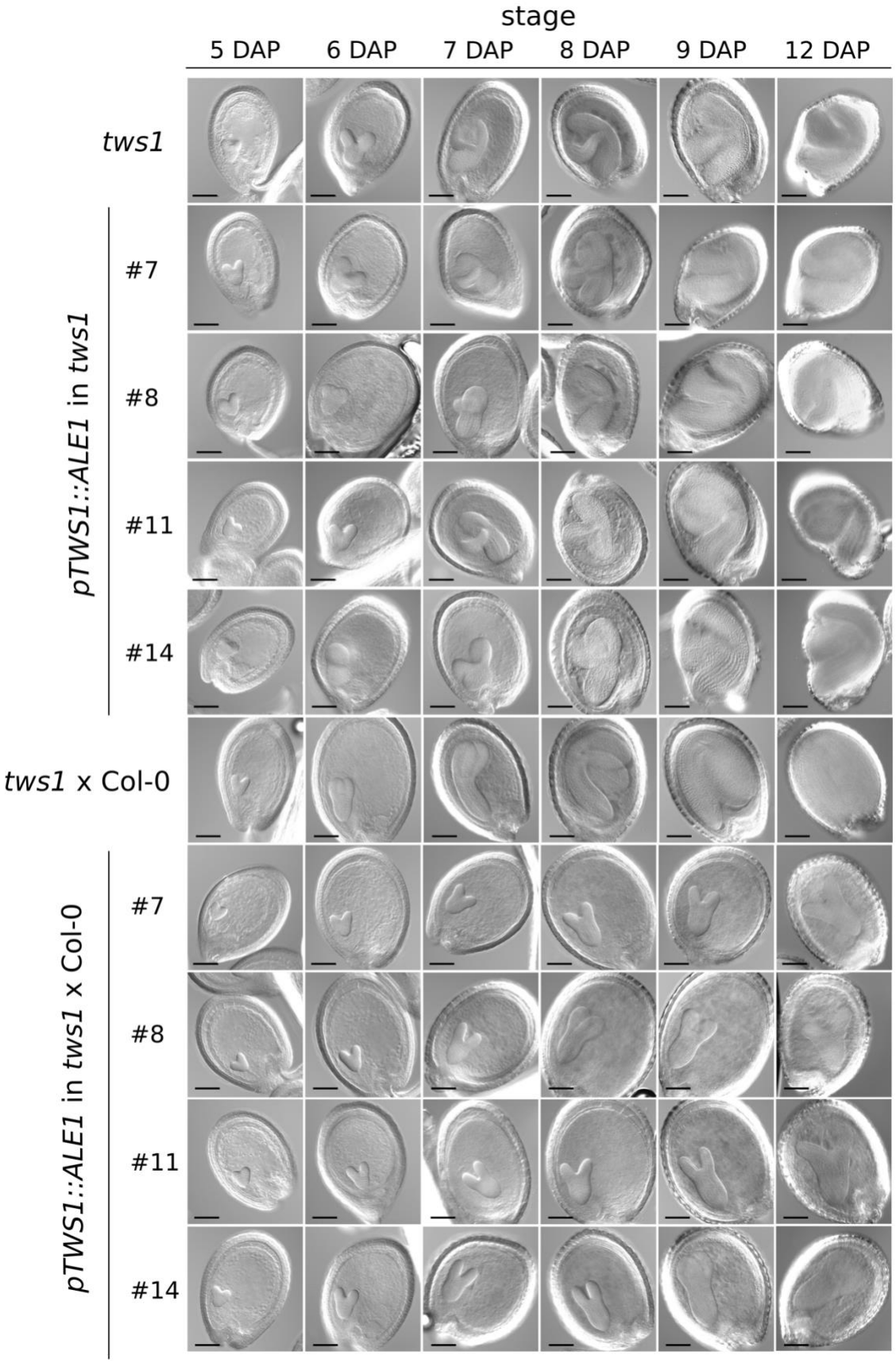
stage
5 DAP
6 DAP
7 DAP
8 DAP
9 DAP
12 DAP
tws1
pTWS1::ALE1 in tws1
#7
#8
#11
#14
tws1 x Col-0
pTWS1::ALE1 in tws1 x Col-0
#7
#8
#11
#14

Fig. S19. Co-expression of ALE1 and TWS1 in the embryo induces severe developmental phenotypes in the embryo. Chloral hydrate staining on seeds at different stages (DAP = Days After Pollination). Genotypes are indicated on the left side of the panel.

A

	tws1 x Col-0	*pTWS1::ALE1* in *tws1* x Col-0			
		#7	#8	#11	#14
% germination	100	51.7%	72,4%	58,8%	57.1%

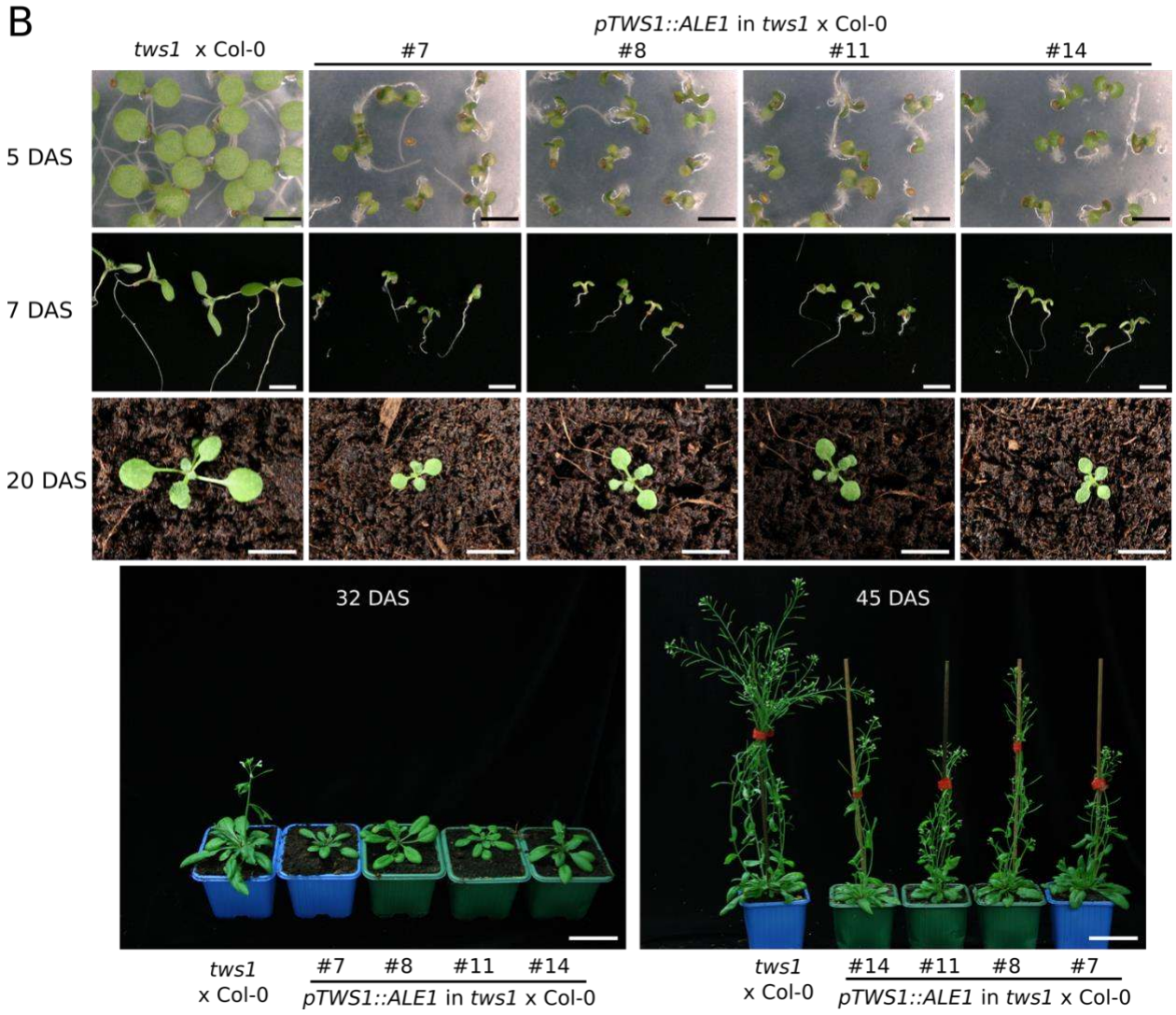

Fig. S20. Co-expression of ALE1 and TWS1 in the embryo retards embryo growth but does not affect post-germination development. A) Percentage of germination in 4 independent populations of seeds from lines carrying *pTWS1::ALE1* in the *tws1-4* background crossed with Col-0 and in control *tws1-4* x Col-0, n>90. B) Plant morphology of seedlings before and at different stages post transplantation to soil for representative individuals from each cross. DAS = days after stratification. Scale bars = 2mm for the two upper lines, = 1cm for the third line, 5cm for the last line.

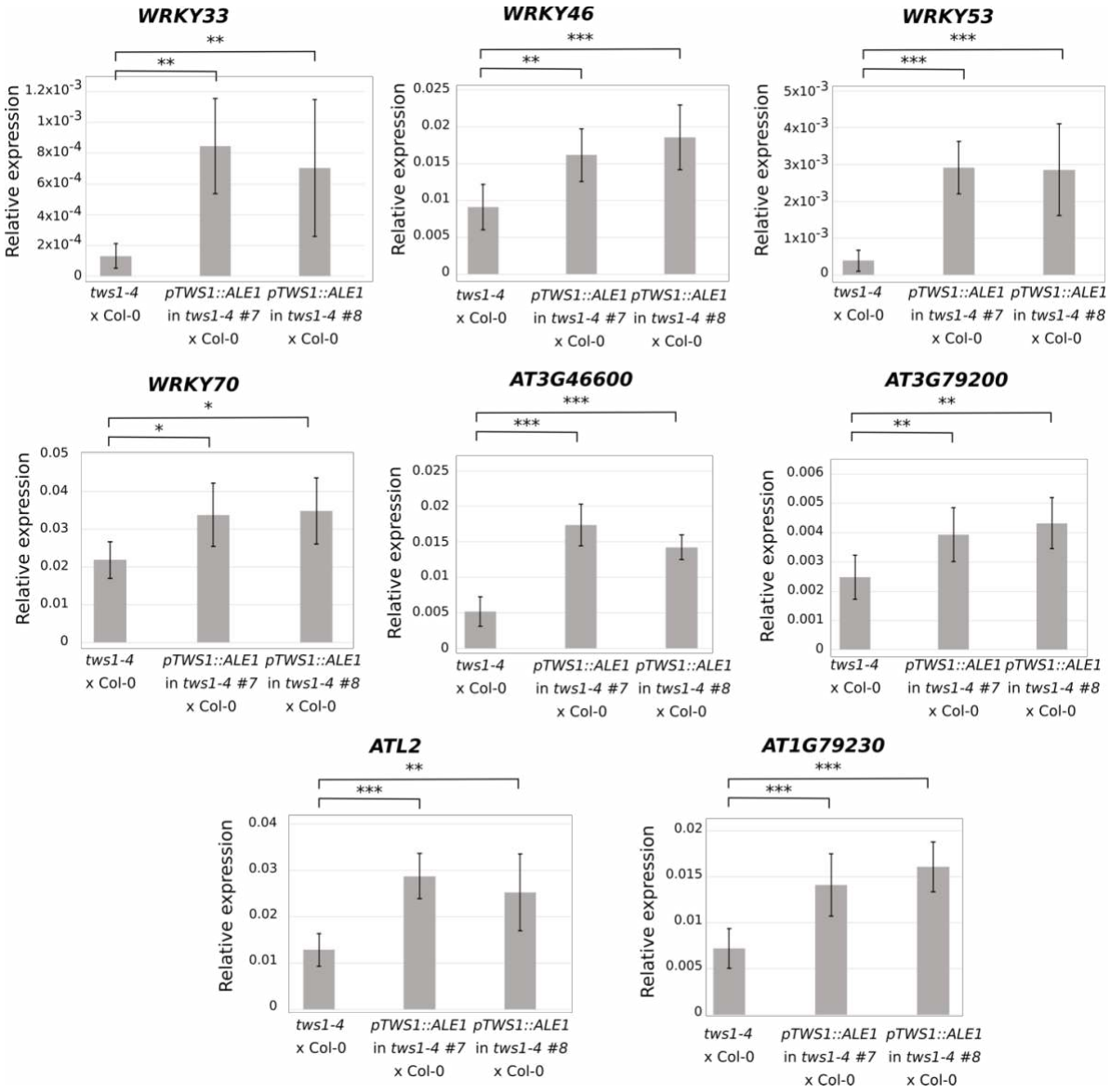

Fig. S21. Co-expression of ALE1 and TWS1 in the embryo upregulates GSO1/GSO2 signalling targets in developing seeds. qRT-PCR on previously identified targets of GSO1/GSO2 signalling in 6 DAP siliques from crosses of Col-0 pollen onto two independent lines expressing *ALE1* in the embryo (*pTWS1::ALE1*) in the *tws1-4* background. Experiments were carried out using 5 biological replicates. Expression values are normalized to the *EIF4A* housekeeping gene. *** indicates $p<0.01$, ** indicates $p<0.05$ and * indicates $p<0.1$ by a one-way ANOVA followed by a Scheffé multiple comparison post-hoc test. Bars indicate standard errors.

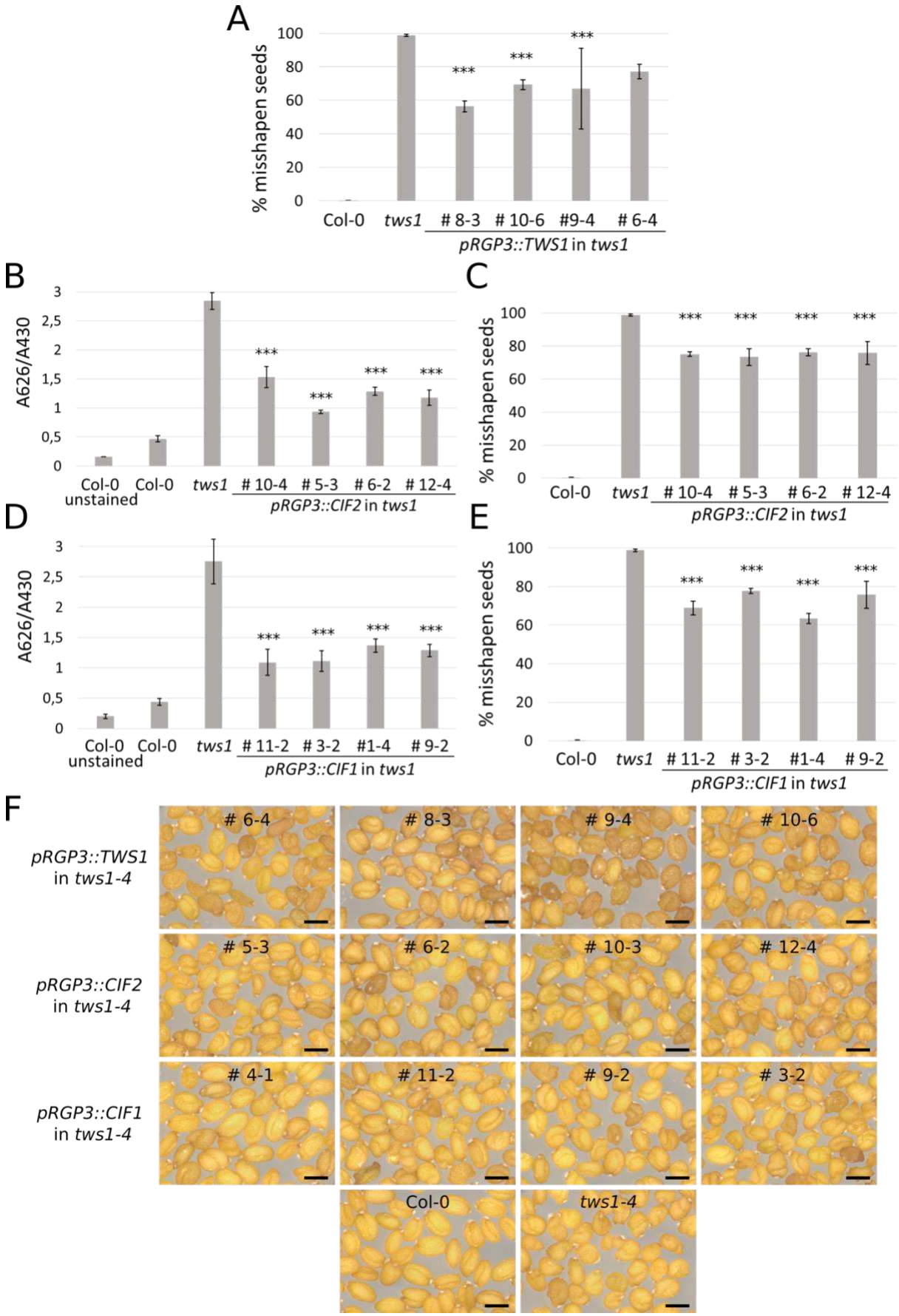
A
% misshapen seeds
100
80
60
40
20
0
***
***
***
Col-0
tws1
8-3
10-6
#9-4
6-4
pRGP3::TWS1 in tws1
B
A626/A430
3
2,5
2
1,5
1
0,5
0
***
***
***
***
Col-0 unstained
Col-0
tws1
10-4
5-3
6-2
12-4
pRGP3::CIF2 in tws1
C
% misshapen seeds
100
80
60
40
20
0
***
***
***
***
Col-0
tws1
10-4
5-3
6-2
12-4
pRGP3::CIF2 in tws1
D
A626/A430
3
2,5
2
1,5
1
0,5
0
***
***
***
***
Col-0 unstained
Col-0
tws1
11-2
3-2
#1-4
9-2
pRGP3::CIF1 in tws1
E
% misshapen seeds
100
80
60
40
20
0
***
***
***
***
Col-0
tws1
11-2
3-2
#1-4
9-2
pRGP3::CIF1 in tws1
F
pRGP3::TWS1 in tws1-4
6-4
8-3
9-4
10-6
pRGP3::CIF2 in tws1-4
5-3
6-2
10-3
12-4
pRGP3::CIF1 in tws1-4
4-1
11-2
9-2
3-2
Col-0
tws1-4

Fig. S22. Complementation of *tws1* mutants by expression of CIF1, CIF2 and TWS1 in the endosperm. A,C,E) Quantification of the number of misshapen seeds. For each line, at least 400 seeds from 4 independent plants were analysed. B,D) Quantification of toluidine blue uptake into the aerial parts of young seedlings, normalized to chlorophyll content. N = 6, ten seedlings per repetition. A) 4 independent transformation events of *pRGP3::TWS1* in *tws1-4* compared to *tws1-4* and Col-0. B-C) 4 independent transformation events of *pRGP3::CIF2* in *tws1-4* compared to *tws1-4* and Col-0, D-E) 4 independent transforming events of *pRGP3::CIF1* in *tws1-4* compared to *tws1-4* and Col-0. *** indicates a statistical difference with p-value < 0.01 compared to the *tws1-4* mutant using one-way ANOVA followed by post-hoc Scheffé multiple comparison. F) Images of seeds for four independent lines of *pRGP3::TWS1* in *tws1-4*, *pRGP3::CIF2* in *tws1-4* and *pRGP3::CIF1* in *tws1-4* and controls Col-0 and *tws1-4.* Scale bar = 400µm.

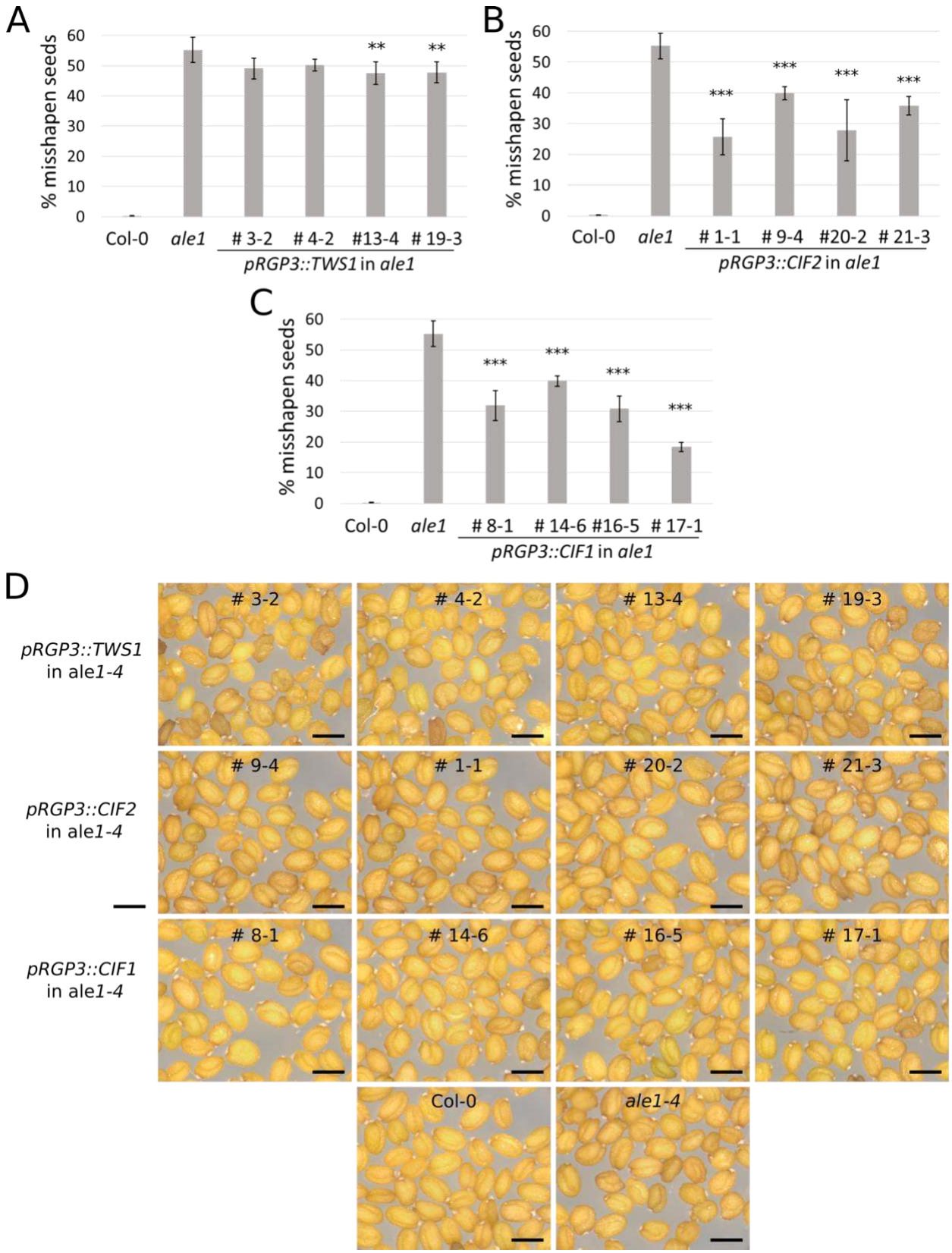

Fig. S23. Complementation of *ale1* mutants by expression of CIF1, CIF2 and TWS1 in the endosperm. A-C) Quantification of the number of misshapen seeds. For each line, at least 400

seeds from 4 independent plants were analysed A) 4 independent transformation events of *pRGP3::TWS1* in *ale1-4* compared to *ale1-4* and Col-0. B) 4 independent transformation events of *pRGP3::CIF2* in *ale1-4* compared to *ale1-4* and Col-0. C) 4 independent transformation events of *pRGP3::CIF1* in *ale1-4* compared to *ale1-4* and Col-0. ***and ** indicate a statistical difference with pvalue<0.01 and pvalue<0.05, respectively for the *tws1* lines expressing the different peptide in the endosperm compared to the *tws1-4* mutant by one-way ANOVA followed by *post-hoc* Scheffé multiple comparison. D) Images of seeds for four independent lines of *pRGP3::TWS1* in *ale1-4*, *pRGP3::CIF2* in *ale1-4* and *pRGP3::CIF1* in *ale1-4* and controls Col-0 and *ale1-4*. Scale bars =400µm